UNIVERSITY OF CRETE

DEPARTMENT OF MATERIALS SCIENCE & TECHNOLOGY

Master Thesis

2D Nanosheets as charge transport layers in perovskite solar cells

Eleni Mantzopoulou

Professor George Kioseoglou

Heraklion, September 2018

Acknowledgments

I would like to thank especially professor Emmanuel Stratakis at Institute of Electronic Structure and Laser (IESL) for the support and help throughout my postgraduate dissertation, professor George Kioseoglou (Department of Materials & Science Engineering) who gave me the opportunity to work with him and advise me throughout the duration of my thesis and professor Emmanuel Kymakis (TEI of Crete) who gave me the chance to work in his laboratory of "Nanomaterials & Organic Electronics (NANO) Group" and interact with excellent people

Abbreviations and Symbols

CdTeSCs	Cadmium Telluride Solar Cells
CIGSSCs	Copper Indium Gallium Selenide Solar Cells
DSSCs	Dye-sensitized Solar Cells
MOSCs	Molecular Organic Solar Cells
PSCs	Perovskite Solar Cells
KRICT	Korea Research Institute of Chemical Technology
NREL	National Renewable Energy Laboratory
V_{oc}	Open circuit voltage
J_{sc}	Short circuit current density
M_{pp}	Maximum Power Point
V_{mp}	Maximum Voltage Point
I_{mp}	Maximum Current Point
J_{mp}	Maximum Current Density Point
FF	Fill Factor
PCE	Power Conversion Efficiency
EQE	External Quantum Efficiency
IQE	Internal Quantum Efficiency
HTL	Hole Transport Layer
HTM	Hole Transport Material
ETL	Electron Transport Layer
TCO	Transparent Conductive Oxide
ITO	Indium Tin Oxide
FTO	Fluorine Tin Oxide
CB	Conduction Band
VB	Valence Band
HOMO	Highest Occupied Molecular Orbital
LUMO	Lowest Unoccupied Molecular Orbital
PEDOT:PSS	Poly(3,4-ethylenedioxythiophene) Polystyrene Sulfonate
PTAA	Poly(bis(4-phenyl)(2,4,6-trimethylphenyl))amine
$PC_{60}BM$	[6,6]-phenyl-C_{60}-butyric acid methyl ester
PFN	Poly[(9,9-bis(3'-(N,N-dimethylamino)propyl)-2,7-fluorene)-alt-2,7-(9,9–dioctylfluorene)]
PbI_2	Lead iodide
MAI	Methyl ammonium iodide
DMF	N,N-Dimethylformamide
GO	Graphene Oxide
rGO	Reduced Graphene Oxide
DMSO	Dimethyl sulfoxide
GBL	γ-Butyrolactone
AFM	Atomic Force Microscopy

TMDs	Transition Metal Dichalcogenides
MoS_2	Molybdenum Disulfide
WS_2	Tungsten Disulfide
WSe_2	Tungsten Diselenide

Περιεχόμενα

Abstract

Metal halide Perovskite Solar Cells are considered the most promising cost-effective photovoltaic technology as they employ ultra-low cost solution-processed semiconductor materials with very unique optoelectronic properties. Additionally, the progress of their PCEs present the steepest rise of any other photovoltaic technology. The perovskite crystalline structure follows the formula ABX3 where A is a small cation, B is a large metal cation, and X is a halogen anion. The two main geometries in which the perovskite solar cells are nowadays constructed are the planar and the inverted one. The layers of the planar or inverted structure are: Anode/Electron Transport Layer/perovskite layer/Hole Transport Layer/Cathode or Anode/Hole Transport Layer/perovskite layer/ Electron Transport Layer/Cathode, respectively. Each material and each layer play a significant part so that the layout to work more effectively.

At this project, we have used the inverted structure because over the years the use of the $PC_{60}BM$ as the Electron Transport Layer reduced the imperfections on the perovskite's surface resulting in negligible hysteresis in the efficiency measurements. Changing the hole transport layer with a 2D dimensional material can result in a higher efficiency due to a better extraction of electrons, higher mobility of charge carries and a better alignment of the energy levels. Two basic materials were used: 1) Graphene Oxide (GO) and 2) Tungsten Disulfide (WS_2) nanosheets fabricated by spin coating and vacuum filtration so that both their surface's uniformity and characteristic values were assessed and tested. In the first case, the reference solar cells were fabricated with PTAA (widespread polymer) as the Hole Transport Material and in second case 2D materials were used for this layer to compare the electrical characteristics of the solar cells. Further characterization of the fabricated structures was performed by using Atomic Force Microscopy (AFM) and UV-visible Spectroscopy.

Περίληψη

Με το πέρασμα των χρόνων, στην τεχνολογία των ηλιακών κυττάρων συνέβησαν αποφασιστικές και αποτελεσματικές αλλαγές με την ανακάλυψη νέων υλικών. Τα οργανικά φωτοβολταϊκά εγκαινίασαν μια περίοδο ανάπτυξης, με χαμηλό κόστος υλικών, με ικανότητα εύκολου χειρισμού και κατασκευής και σημαντικές βελτιώσεις στις χαρακτηριστικές δομές τους. Ένα υλικό, το οποίο έχει σημαντικές ιδιότητες είναι ο περοβσκίτης. Η δομή του είναι ABX_3 όπου στην θέση έχουμε Α: μόλυβδο (Pb) ή κασσίτερο (Sn), Β: μεθυλαμμώνιο (MAI) , Χ: αλογόνα (Cl,Br,I). Ο περοβσκίτης επέφερε με τα πλεονεκτήματα του σπουδαίες ανακαλύψεις στην ερευνητική κοινότητα. Ωστόσο το μεγαλύτερο μειονέκτημα του, πέρα από την τοξικότητα, η σταθερότητα του επειδή επηρεάζεται από την υγρασία του ατμοσφαιρικού αέρα. Δυο βασικές δομές των ηλιακών κυττάρων περοβσκίτη που κατασκευάζονται σήμερα είναι: 1) κανονική ή επίπεδη και 2) ανεστραμμένη. Η επίπεδη δομή είναι άνοδος/στρώμα μεταφοράς ηλεκτρόνιων/στρώμα περοβσκίτη/στρώμα μεταφοράς οπών/κάθοδος και η ανεστραμμένη δομή είναι άνοδος/ στρώμα μεταφοράς οπών/στρώμα περοβσκίτη/στρώμα μεταφοράς ηλεκτρονίων/κάθοδος των οποίων η διάταξη επηρεάζεται από τα ενεργειακά επίπεδα των υλικών. Κάθε υλικό και κάθε στρώμα διαδραματίζει έναν σημαντικό ρόλο ώστε να λειτουργεί πιο αποδοτικά η διάταξη. Στην συγκεκριμένη εργασία, χρησιμοποιήθηκε η ανεστραμμένη δομή λόγω των υλικών που ήδη υπάρχουν και λόγω του στρώματος περοβσκίτη. Με την εναπόθεση του υλικού μεταφοράς ηλεκτρονίων, το φουλερένιο, $PC_{60}BM$, παρατηρήθηκε ότι με την πάροδο του χρόνου, καλύπτονται οι ατέλειες στην επιφάνεια του περοβσκίτη και υπάρχει αμελητέα υστέρηση. Για καλύτερες αποδόσεις ηλιακών κύτταρων έγινε η αλλαγή του υλικού που χρησιμοποιείται για το στρώμα μεταφοράς οπών, με δισδιάστατα υλικά τα οποία είναι ημιαγωγοί με πολύ καλές ιδιότητες όπως η κινητικότητα φορέων και καλύτερη εξαγωγή ηλεκτρονίων σε συνάρτηση με τα ενεργειακά τους επίπεδα. Χρησιμοποιήθηκαν 2 βασικά υλικά: 1) Οξείδιο του γραφενίου και 2) βολφράμιο σουλφίδιο, οπού κατασκευάστηκαν με εναπόθεση περιστροφής και με διήθηση κενού του διαλύματος, ώστε να αξιολογηθεί και να ελεγχθεί η ομοιομορφία των επιφανειών τους και τα χαρακτηριστικά μεγέθη. Η σύγκριση αυτών έγινε μεταξύ των βασικών δομών ηλιακών κυττάρων με την χρήση του υλικού μεταφοράς οπών, στην πρώτη περίπτωση, το πιο διαδεδομένο πολυμερές, PTAA και στην δεύτερη περίπτωση, με την χρήση των δισδιάστατων υλικών. Για περαιτέρω χαρακτηρισμό των πειραματικά κατασκευασμένων υλικών χρησιμοποιήθηκαν οι τεχνικές Μικροσκοπία Ατομικής Δύναμης και Φασματοσκοπία Υπεριώδους-Ορατού.

1.Introduction

1.1 Solar energy

Every day, the sun radiates an enormous amount of energy as called solar energy. It radiates more energy in one day than the world uses in one year. This energy comes from within the sun itself. Like most stars, the sun is a big gas ball made up mostly of hydrogen and helium gas. The sun makes energy in its inner core in a process called nuclear fusion. It takes the sun's energy just a little over eight minutes to travel the 93 million miles to Earth. Solar energy travels at the speed of light, or 186.000 miles per second, or 3.0 x 10^8 meters per second. Only a small part of the visible radiant energy (light) that the sun emits into space ever reaches the Earth, but that is more than enough to supply all our energy needs. Solar energy is considered a renewable energy source due to this fact. Today, people use solar energy to heat buildings and water and to generate electricity. Solar energy is mostly used by residences and to generate electricity. The most technologies that are currently exploiting solar energy are the solar collectors, solar space heating, solar water heating, photovoltaics and solar thermal systems. Electricity is produced when radiant energy from the sun strikes the solar cell, causing the electrons to move around. The action of the electrons starts an electric current. The conversion of sunlight into electricity takes place silently and instantly. There are no mechanical parts to wear out. Compared to other ways of making electricity, photovoltaic systems are expensive and many panels are needed to equal the electricity generated at other types of plants.

1.2 Photoelectric effect

The photoelectric effect is the emission of electrons from a metal caused by light or ultraviolet rays on the surface. The emission of electrons occurs only when its frequency radiation is greater than a limit value. The energy of "photoelectrons" does not depend on its intensity radiation but only by its frequency. The quantum interpretation of this effect is derived from the following definitions and types. The electromagnetic wave is composed from photon energy E = $h*f$. Einstein's photoelectric equation: $h * f = W + K$ where W is the work extraction of metal and K is the kinetic energy of photoelectrons. For the extraction must apply h*f ≥ W.

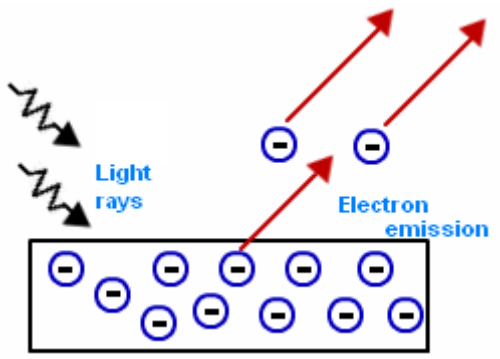

Figure 1: Schematic of the interpretation of the photoelectric effect

1.3 Solar cells

The solar cell is an electrical device converts the energy of light directly to electrical energy by the photovoltaic effect, which is a physical and chemical phenomenon. It is a form of photoelectric cell, defined as a device whose electrical characteristics, such as current, voltage, or resistance, vary when exposed to light. Solar cells are the building blocks of photovoltaic modules, otherwise known as solar panels. Solar cells are described as being photovoltaic irrespective of whether the source is sunlight or an artificial light. They are used as a photo detector (for example infrared detectors), detecting light or other electromagnetic radiation near the visible range, or measuring light intensity. The operation of a photovoltaic cell consists 3 basic features:

1. The absorption of light, generating either electron-hole pairs.
2. The separation of charge carriers of opposite types.
3. The separate extraction of those carriers to an external circuit.

1.4 Types of solar cells

Solar cells can be made of only one single layer of light-absorbing material (single-junction) or use multiple physical configurations (multi-junctions) to take advantage of various absorption and charge separation mechanisms. Solar cells can be classified into first, second and third generation cells.

The ***first generation*** cells also called conventional, traditional based cells. The main advantage of these solar cells is the very high efficiency when the theoretical maximum power conventional efficiency is 29% but the most importantly disadvantage is the cost of the production for solar cell. In the first generation of solar cells included materials that are based on silicon such as monocrystalline, polycrystalline, amorphous and hybrid silicon.

***Monocrystalline Silicon Cells*:**

They are the original materials for the photovoltaic technology invented in 1955. The modules of single crystal composed of cells cut from a piece of continuous crystal. The material forms a cylinder which is sliced into thin circular wafers. To minimize waste, the cells may be fully round or they may be trimmed into other shapes, retaining more or less of the original circle. Because each cell cut from a single crystal, it has a uniform color, which is dark blue.

Polycrystalline Silicon Cells:

They are made from similar silicon material except that instead of being grown into a single crystal, they are melted and poured into a mold. This forms a square block that can be cut into square wafers with less waste of space or material than round single-crystal wafers. As the material, is crystallized in an imperfect manner, forming random crystal boundaries. The power conversion efficiency is slightly lower, that

means the size of the finished module is slightly greater per watt than most single crystal modules. The cells look different from single crystal cells. The appearance of surface with many variations has blue color. In fact, they are quite beautiful like sheets of gemstone.

Crystalline silicon solar cells derive their name from the way they are made and Polycrystalline cells are made by melting the silicon but, the difference between monocrystalline and polycrystalline solar panels is that monocrystalline cells are cut into thin wafers from a singular continuous crystal that has been grown for this purpose.

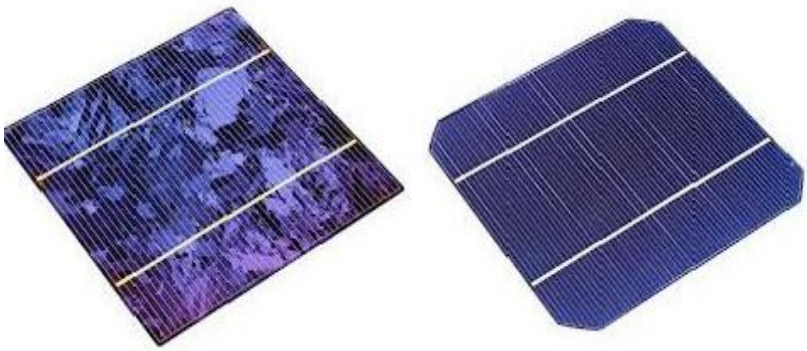

Figure 2: Device of polycrystalline silicon solar cell (left) and monocrystalline silicon solar cell (right)

Amorphous Silicon Cells:

Instead of growing silicon crystals as is done in making the two previous types of solar cells, silicon is deposited in a very thin layer on to a backing substrate – such as metal, glass or even plastic, with many applications in everyday devices (e.g. calculators, small electronic devices etc.) Sometimes several layers of Si, doped in slightly different ways to respond to different wavelengths of light, are laid on top of one another to improve the efficiency. The production methods are complex, but less energy intensive than crystalline panels and prices have been coming down as panels are mass-produced using this process.

One advantage of use very thin layers of silicon is that the panels can be made flexible. The disadvantage of amorphous panels is that they are much less efficient per unit area and are generally not suitable for roof installations you would typically need nearly double the panel area for the same power output. However, there flexibility makes them an excellent choice for use for fabrication integrated photovoltaic (e.g., roofing shingles), for use on curved surfaces, or even attached to a flexible backing sheet so that they can even be rolled up and used when going backpacking, or put away when they are not needed.

Hybrid Silicon Cells:

One recent trend in the industry is the emergence of hybrid silicon cells and several companies are now exploring ways of combining different materials to make solar cells with better efficiency, longer life, and at reduced costs. Recently, Sanyo introduced a hybrid cell whereby a layer of amorphous silicon is deposited on top of single crystal wafers. The result is an efficient solar cell that performs well in terms of indirect light and is much less likely to lose efficiency as the temperature increases

.

- The ***second generation*** cells are thin film solar cells, that include CdTe and CIGS cells and are commercially significant in utility-scale photovoltaic power stations, building integrated photovoltaics or in small standalone power system.

Cadmium Telluride Solar Cells (CdTe):

Describe a photovoltaic technology that is based on the use of cadmium telluride, a thin semiconductor layer designed to absorb and convert sunlight into electricity. Cadmium telluride photovoltaic is the only thin film technology with lower costs than conventional solar cells made of crystalline silicon in multi-kilowatt systems. Over the years, the lifetime of CdTe cells have the lowest comprehensiveness of carbon, lowest water use and shortest energy payback time of all solar technologies. The toxicity of cadmium is an environmental concern mitigated by the recycling of CdTe modules at the end of their life time, though there are still uncertainties and the public opinion is skeptical towards this technology.

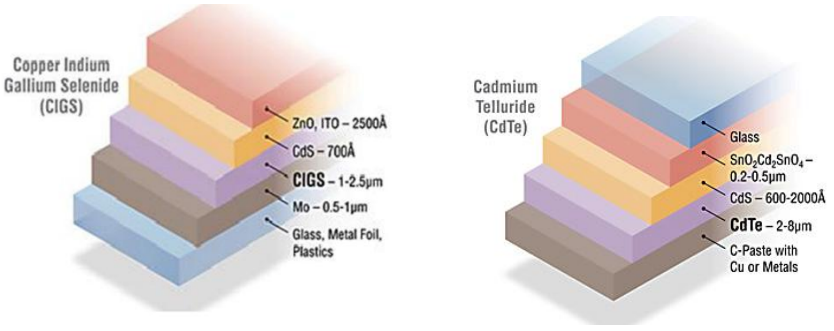

Figure 3: The structures for five layers that comprise CdTe and CIGS solar cells, respectively

Copper Indium Gallium Selenide Solar Cells (CIGS):

One of the most interesting and controversial materials in solar is Copper-Indium-Gallium-Selenide, or CIGS for short. A copper indium gallium selenide solar cell is a thin film solar cell used to convert sunlight into electric power. They are manufactured by depositing a thin layer of copper, indium, gallium and selenide on glass or plastic backing, along with electrodes on the front and back to collect current. Because the material has a high absorption coefficient and strongly absorbs sunlight, a much thinner film is required than of other semiconductor materials. CIGS is one of three mainstream thin-film PV technologies, the other two being cadmium telluride and amorphous silicon. Like these materials, CIGS layers are thin enough to be flexible, allowing them to be deposited on flexible substrates. However, as all of these technologies normally use high-temperature deposition techniques, the best performance normally comes from cells deposited on glass. Even then the performance is marginal compared to modern polysilicon-based panels. Advances in low-temperature deposition of CIGS cells have erased much of this performance difference. It is best known as the material for CIGS solar cells a thin-film technology used in the photovoltaic industry. In this role, CIGS has the advantage of being able to be deposited on flexible substrate materials, producing highly flexible, lightweight solar panels. Improvements in efficiency have made CIGS an established technology among alternative cell materials.

The ***third generation*** of solar cells includes a number of thin-film technologies often described as emerging photovoltaics—most of them have not yet been commercially applied and are still in the research or development phase. A generation beyond silicon-based solar cells. Specifically, 3G includes solar cells which do not use the p-n junction structure that is used in traditional semiconductor, Si-based solar cells. The 3G generation contains a wide range of potential and efficient solar innovations including: Dye-sensitized solar cells (DSSCs), molecular organic solar cells (MOSCs), polymer organic solar cells (POSCs) and perovskite solar cells (PSCs).

Dye-Sensitized Solar Cells (DSSCs):

These type of solar cells also sometimes referred to as dye sensitized cells (DSC), are a third generation photovoltaic (solar) cell that converts any visible light into electrical energy. This new class of advanced solar cell can be likened to artificial photosynthesis due to the way in which it mimics nature's absorption of light energy. DSSC is a disruptive technology that can be used to produce electricity in a wide range of light conditions, indoors and outdoors, enabling the user to convert both artificial and natural light into energy to power a broad range of electronic devices. A dye-sensitized solar cell is a low-cost solar cell belonging to the group of thin film solar cells. It is based on a semiconductor formed between a photosensitized anode and an electrolyte, a photo electrochemical system. The DSSCs have interesting features: 1) is simple to make using conventional roll-printing techniques,2) is semi-flexible and semi-transparent which offers a variety of uses not applicable to glass-

based systems, and 3) most of the materials that used are low cost. In practice it has proven difficult to eliminate a number of expensive materials, notably platinum and ruthenium, and the liquid electrolyte presents a serious challenge to making a cell suitable for use in all weather. Although power conversion efficiency is less than the best thin films, in theory its price/performance ratio should be good enough to allow them to compete with fossil fuel electrical generation.

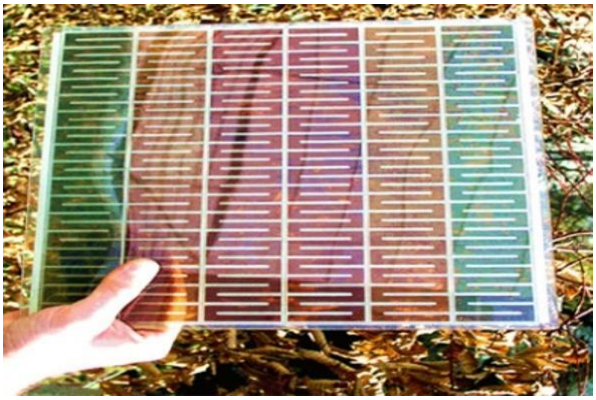

Figure 4: Device of a dye-sensitized solar cell

Molecular Organic Solar Cells:

Small molecular semiconductors can be generally classified as hole or electron transporting (p-type or n-type) materials according to the type of orderly transferring charge carriers, under a given set of conditions, stemming from removal of electrons from the filled molecular orbitals or from the addition of electrons to empty orbitals, respectively. Many small molecular p-type semiconductors have been studied for decades. Among these molecules, only a small fraction has been applied successfully as electron donors in OPV devices due to the various optical, electrical, and stability requirements demanded of the chosen materials. The properties of materials, such as hole mobility (i.e., the distance over which holes are transported per second under the unit electric field), exciton diffusion length, thin film morphology, energy level alignment, band gap and absorption coefficient, all greatly affect the performance of OPV device. In this section, some representative small molecular donors such as dyes, fused acenes, oligothiophenes, and triphenylamine-based molecules used in the active layer of OPVs.

Polymer Organic Solar Cells:

The organic solar cells technologies are under continuous development as that interest stems from their great characteristics including: fabrication with flexible substrates, lightweight, and production by inexpensive, low temperature deposition techniques such as spin-coating and printing, solution processed, transparent and use of cheap

raw materials. Contemporary OPVs are based on a heterojunction resulting from the contact of an electron donor (D) and an electron acceptor (A) material.

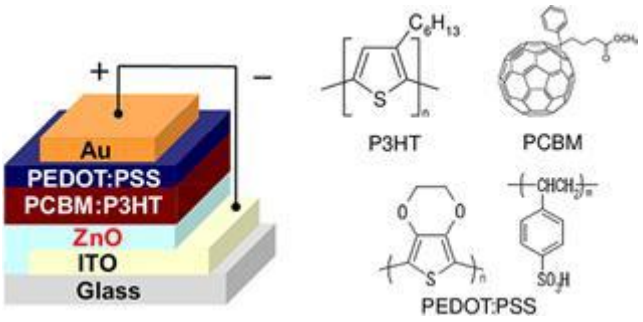

Figure 5: The structure of polymer solar cell in which use electron donor & acceptor

Absorption of solar photons creates exciton, which diffuse to the D/A interface, where they are dissociated into free holes and electrons, and opposite polarity carriers (holes and electrons) transport through the donor and acceptor channels to anodes and cathodes respectively, charges are collected at the electrodes, resulting in the generation of electrical power. There are three categories of polymer organic solar cells:

1. ***Single layer:*** These type of solar cell is the simplest of all for the organic solar cells. A single layer of single component organic material was sandwiched between two different electrodes with different work functions. In these single layer, the built-in potential is derived from either a Schottky-type potential barrier at one of the metal/organic contacts or the difference in work function of the electrodes, and the photovoltaic properties are strongly dependent on the nature of the electrodes. These early OPVs showed very poor performance.
2. ***Bilayer heterojunction:*** The architecture has been intensively investigated and still is an invaluable tool for the evaluation of new active materials, nevertheless, performance of OPVs based on this structure is limited by the short exciton diffusion length in organic materials (typically 5–20 nm). Since the exciton dissociation process is confined to the D/A interfacial zone, only excitons produced at a distance shorter than their diffusion length have a good probability to reach the interfacial zone and generate free charge carriers. So the exciton diffusion length limits the maximum thickness of the active layer and thus the maximum fraction of the incident light that the cell can absorb and covert into electricity.
3. ***Bulk heterojunction:*** is a blend of bicontinuous and interpenetrating donor and acceptor components in a bulk volume. Such a nanoscale network exhibits a D/A phase separation in a 5–20 nm length scale, which is within a distance less than the exciton diffusion length. Compared to bilayer heterojunction,

BHJ significantly increases the D/A interfacial area, leading to enhanced efficiency of the OPV devices.

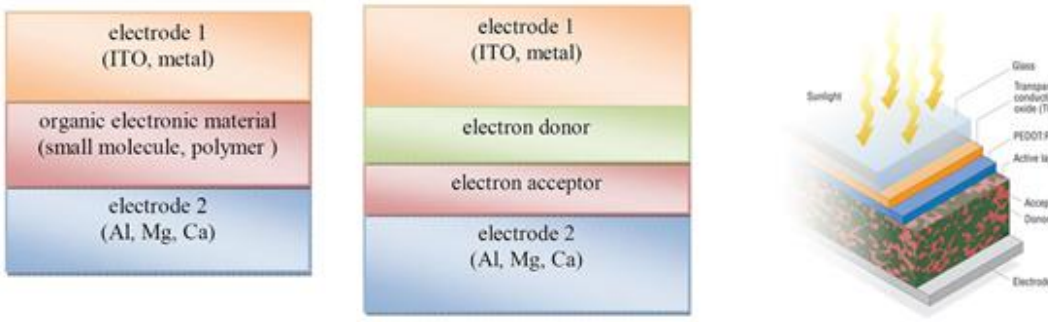

Figure 6:The structure of bulk heterojunction

2. Perovskite solar sells

2.1 History of perovskite

The perovskite mineral was discovered by Gustav Rose in 1839 and is named after Russian mineralogist Count Lev Alekseevich Perovski (1792-1856). The perovskite material is derived from calcium titanate ($CaTiO_3$) compound, which has the molecular structure of the type ABX_3. These materials used in solar cells are a kind of organic-inorganic metal halide compound with perovskite structure, in which group A (methyl ammonium, $CH_3NH_3^+$, MA^+ or formamidinium, $CH(NH_2^+)$, FA^+ is located at the center of the cubic lattice, the metal cation B (Pb^{2+}, Sn^{2+}) and halogen anion X (Br^{-1}, Cl^{-1}, I^{-1} or a coexistence of several halogens) occupy the core and apex of the octahedra, respectively. The metal-halogen octahedra are joined together to form a stable three dimensional structure.

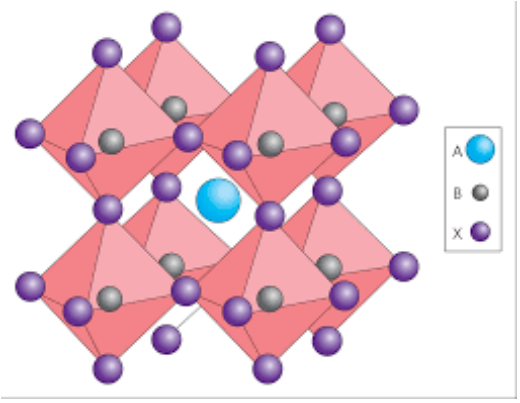

Figure 7: The typical structure of perovskite material with type ABX_3

The kind of these materials have attracted wide an attention because of the cubic lattice-nested octahedral structures and the unique electrical, optical, thermal and other properties.

2.2 Historical evolution

In early 2013, the KRICT researchers discovered a new technology from a new mineral and organic hybrid perovskite material. Recently, have developed a structure and the manufacturing technology, for the organic hybrid perovskite solar cell, which are given the most efficient solar cell in the world, with the power conversion efficiency rate of 17.9 percent. The NREL researchers have concerned with the efficiency of perovskite solar cell for two years, with the result to increase the efficiency from 16.2 percent in 2013 to 17.9 percent in 2014. Also reducing the cost of production to one third that of existing silicon based cell production cost. The aim of all these is, in coming years to become the massive commercialization of perovskite solar cells to have equally good power conversion efficiency and at the same time belong to a more economical generation of solar cells.

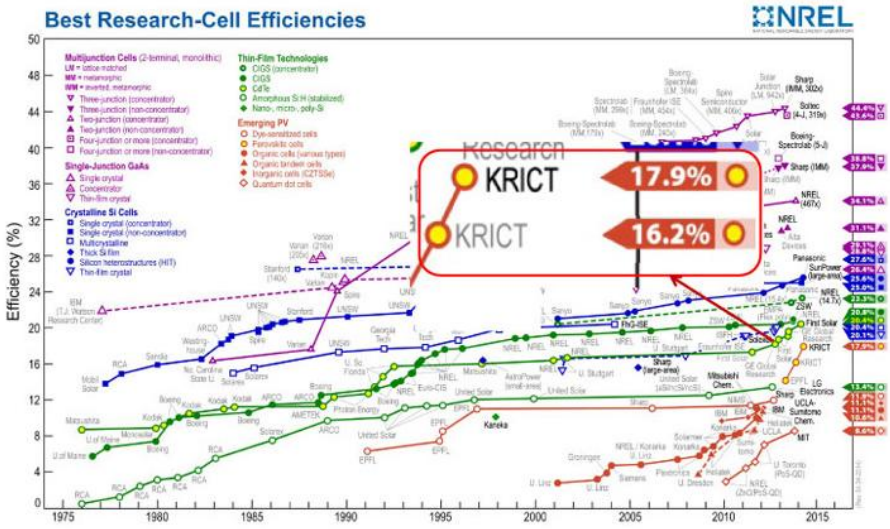

Figure 8: The map with the best research cell efficiencies

2.3 Properties of perovskite solar cells

The properties of the materials involved in the manufacture of perovskite solar cells play an important role in the characterization of a successful device. The separation of these properties has to do either with the chemical or physical properties of the materials that have been taken up or with the treatment of those that have the effect of influence the characteristics of the solar cell, especially its efficiency. The advantages of perovskite solar cells are:

- ***Low cost solution processing materials***
  All of the materials used to manufacture a solar cell are in solutions that are easy to synthesize and process to fabricate the layers of solar cell.

Figure 9: The solutions of the materials of perovskite solar cells

- ***Tunable bandgap***
  The bandgap of perovskite solar cells can be changed through modifying the synthesis of the perovskite material, which is very useful for the application for the solar cells. For example, when replacing MA cation (2.70Å) with Cs^+ ion (1.81Å) in perovskite structure $MAPbI_3$, has a result the increase for the bandgap from 1.55eV to 1.73eV, due to size of the atoms.

- ***High electron, hole mobilities and diffusion lengths***
  One of the most important characteristics of perovskite is the high diffusion length and the high carrier mobility. Regarding with the reported values for the carrier mobility and diffusion length are 66 $cm^2V^{-1}s^{-1}$ and ~1.9μm respectively and the carrier concentration of ~ 10^9 cm^{-3}, due to the lack of deep trap-states.

- ***Free photo-generated carriers***
  The exciton binding energy is a main element to generate photovoltaics actions in perovskite solar cells. Theoretically, a photoexcitation can excite the electrons from valance band (VB) to the conduction band (CB), thus forming conduction electrons when the photon energy exceeds the bandgap in semiconductors. The conduction electrons can undergo two processes, either transport towards generating free charge carries driven by a built-in field or a relaxation towards forming excitons through a multiphoton process. More specifically in $CH_3NH_3PbI_3$ the exciton binding energy has been reported (~37meV) and therefore it's comparable with the thermal energy at room temperature (K_BT=26meV). Therefore, perovskites are non excitonic materials and can generate carrier upon illumination.
- ***Strong optical absorption***
  The large absorbance coefficients in the visible spectrum reveals $CH_3NH_3PbI_3$ perovskite due to direct bandgap as shown in Figure 10.

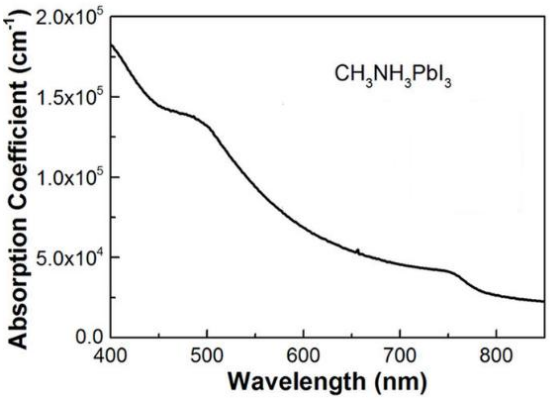

Figure 10 : The absorption coefficient of $CH_3NH_3PbI_3$

However, the important advantages of perovskite solar cells, there are some disadvantages which affect the typical sizes of solar cells and especially the power conversion efficiency.

- ***Toxicity***
  A typical structure of perovskite solar cell uses Pb (lead) as a main material for synthesis perovskite products. The lead is known to be toxic and the presence of lead to perovskite solar cell effect negatively on the environment during the fabrication solar cells or the release of Pb compounds into the environment after of a failed fabrication solar cell.
- ***Stability***
  The instability of perovskite solar cells is an important factor which results in the non- commercialization of this category of solar cells. They are negatively affected when interact with head, light and water. The significant influence on the instability of solar cells has the perovskite- like material which is unstable but also the materials used for electrons or holes transport, in the device architecture and leads to rapid degradation. For example, the most common materials that are used in the hole transport layer (HTL) and electron transport layer (ETL) are PEDOT: PSS and PCBM. The PEDOT: PSS layer has hydroscopic behavior and has acidic nature (pH~2) affected the stability of the device and PCBM layer is not stable in the air.

- ***Hysteresis***
  The hysteresis phenomena observed in the J-V characteristic curve of perovskite solar cells. The hysteresis behavior has been explained with several mechanisms such as: capacitive effects, ion migration, charge trapping, ferroelectric polarization, charge accumulation at the interfaces or unbalanced distribution of electrons and holes. In the typical hysteresis is the reverse scan current e.g. measured by reducing the voltage from open circuit bias (V_{oc}) to short circuit, is larger than in the forward scan. The scanning direction is

called as backward or reverse scan when the voltage is swept from positive (open circuit) to negative (short circuit), whereas the scan in the opposite direction is termed as forward scan. Therefore, hysteresis imposes a serious problem on the accurate determination of perovskite solar cell efficiencies and long term device operational stability.

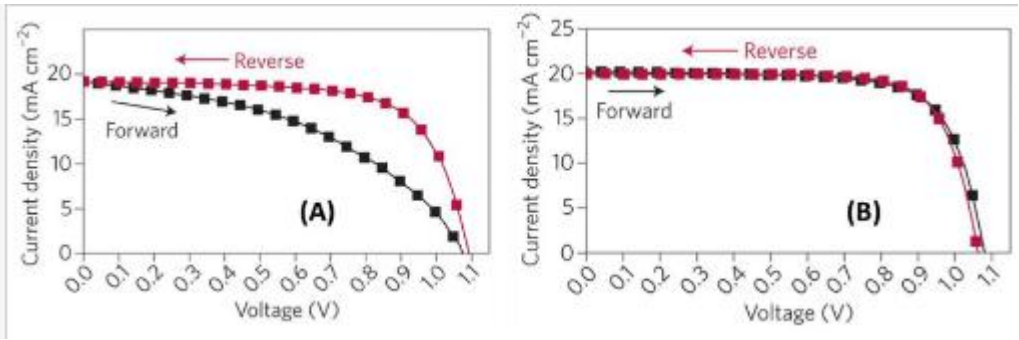

Figure 11: A) The I-V curve response with hysteresis B) The negligible hysteresis in PSCs

3. Operation principles solar cells

3.1 Operating Mechanism

1. **Photon absorption**
   The first step is the absorption of the light from the semiconductor, this results in an excited state of electrons. The electrons are excited to the CB leaving behind positive holes in the VB. The VB is the highest range of electron energies in which electrons are usually found at 0K temperatures. On the other hand, the CB is the range of energy needed to free an electron from an atom and turn it into a delocalized electron that can move freely in the atomic lattice. The absence of an electron, is called a hole and behaves as a positive charge.
2. **Separation of exciton**
   The electron - hole pair created is called exciton. The excess energy will be lost in the form of heat. Electrons can move from the valence band to conduction band through absorbing photons of energy equally or a little bit higher that the difference in energy among VB and CB (excitation). The energy between these bands is called the band gap (E_g). Most organic semiconductors have an energy gap E_g ~ 2eV, which is much higher than silicon (E_g = 1.1 eV). This results in
   to absorb a stronger percentage of incoming solar radiation.
3. **Separation of charge carries**
   After the exciton creation takes place electron-hole separation. Separation can take place at the semiconductor interface with the metal, in contaminated areas, or between the two materials that have a sufficient difference in electron and ionization energies. Once electrons and holes are photo-generated in the perovskite absorber, they are separated at the carrier selective layer contacts as

each of them blocks one type of carrier and lets the other one to transmit through electrode. An electron selective layer transports electrons and blocks holes as such, it is called the electron-transport layer (ETL), or hole blocking layer. Likewise, a hole-transport layer (HTL) transports holes and blocks electrons

This happens due to the fact that energy level of ETL and HTL is lower in the CB and higher in the VB than that of the perovskite's respectively.

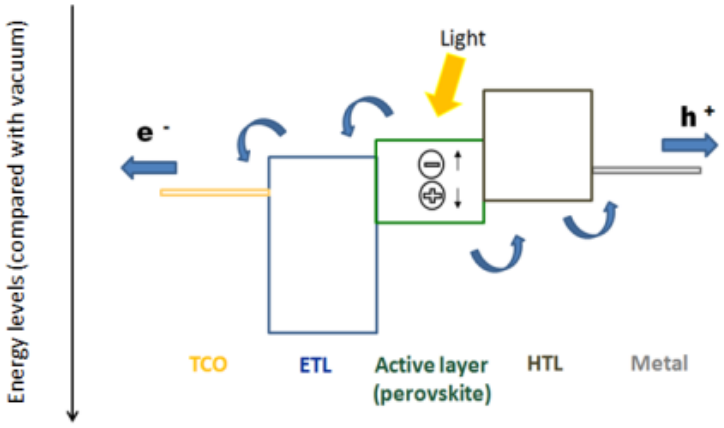

Figure 12: The generation and separation of carries by HTL and ETL

4. **Charge carriers transport**
   After separation of the exciton, transferred the two opposite charges to the electrodes. Transport is affected by reconnecting them and thus resulting in the simultaneous emission of radiation. Electrons travel to the anode and holes travel to the cathode generating a current and a potential difference, which can be harnessed into electricity.
5. **Charge collection**
   The charge collection is done with the help of an electrode with a small work function as the electron collection electrode and a transparent one electrode with a large work function as a hole collection electrode. As a result, a potential difference is created between the terminals of the passage sections. The correct selection of the electrodes is very important for their successful operation for solar cells. As a work function, W_f is defined as the energy required to transfer an electron from the Fermi level (E_f) level to an infinite distance from it.

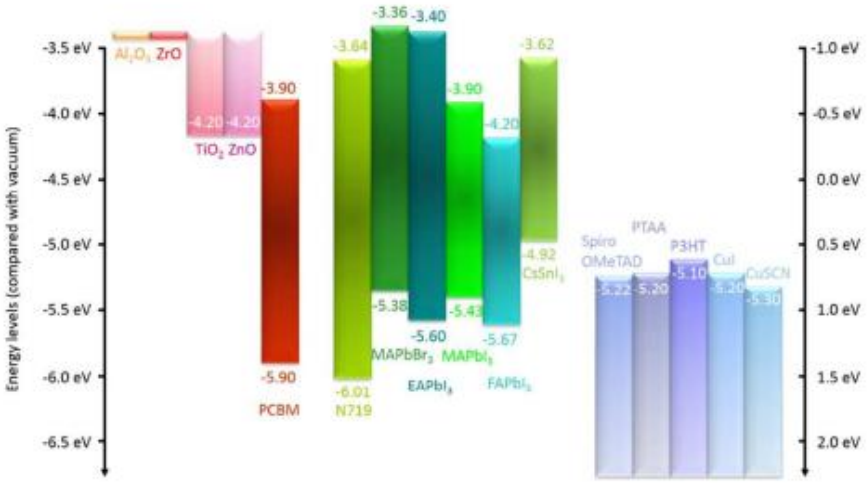

Figure 13: Energy level with different materials as HTL (right), perovskite absorbers (middle) and ETL (left)

3.2 Semiconductors

The semiconductors are a category of solid materials characterized by a small number of free electrons as opposed to the metals they present a large number of free electrons and insulators that have little free electrons. Another important difference in these three categories of solids is that associated with the values that showed the energy gap (E_g), between conduction band and valence band.

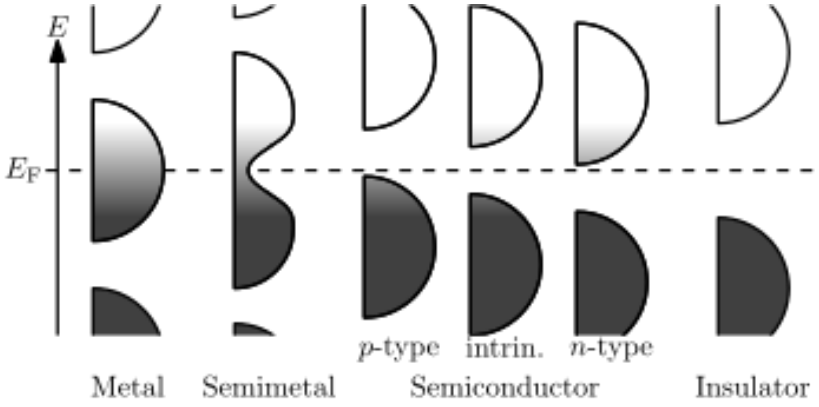

Figure 14: Conduction and valance bands for solid materials

In the above Figure shows the relative position of the valence and conduction bands for the categories of solids materials. In conductors (zero energy gap) is easy the transfer of electrons from the valence band to the conduction band. In semiconductors though, if the valence electrons absorb energy, it is possible to overcome the energy gap E_g which does not have very high values (~1eV), to enter the conduction band and become free electrons (e^-). The empty spaces which in the valence band called holes

(h^+). In the insulators are almost impossible the transition one of the valence electrons to the conduction band, due to high E_g values (~5eV). In the following table, the conductivity properties of the materials are presented.

Table 1: Electrical Properties of materials

Materials	***Specific resistance ρ (Ωhm*cm)***	***Conductivity σ (S/cm)***
Insulators	10^{18}-10^{8}	10^{-18}-10^{-8}
Semiconductors	10^{8}-10^{-3}	10^{-8}-10^{3}
Conductors	10^{-3}-10^{-8}	10^{3}-10^{8}

On the other hand, the semiconductors separated in 2 more categories depending on dopant species. The first category is ***intrinsic semiconductor***, also called undoped or i-type semiconductor, which is a pure semiconductor without any significant dopant species. In this case, there are no charge carries to 0˚K. if the temperature increases there will be carries due to thermal stimulation: electrons will acquire enough energy due to the heat, so from valence band rise to conduction band leaving at the same time a gap (hole) in the valence band. Where it is obvious, that the concentration of electrons (n) and the concentration of the holes (p) are equal to the intrinsic semiconductors. The most common semiconductors for this category is Germanium (Ge) and silicon (Si).

For example, the atom of Ge consists of the core with 32 protons around which they rotate 32 electrons. The valence electrons which are in the outer layer is 4. Each Germanium atom contributes each of the 4 electrons in a corresponding neighboring atom and thus forming covalent bonds that keep the atoms together in crystalline lattice. Therefore, when the temperature of the semiconductor is close to absolute zero the valence electrons are retained in this covalent bonds, while, when the temperature rises it is possible to switch some electrons to the conduction band by overcoming the energy gap. This way creates free electrons in the conduction band and corresponding holes in the valence band with loads (h^+) each. When an electric field is applied to the semiconductor, not only the electrons of the conduction band will be moved but also the holes in the opposite direction.

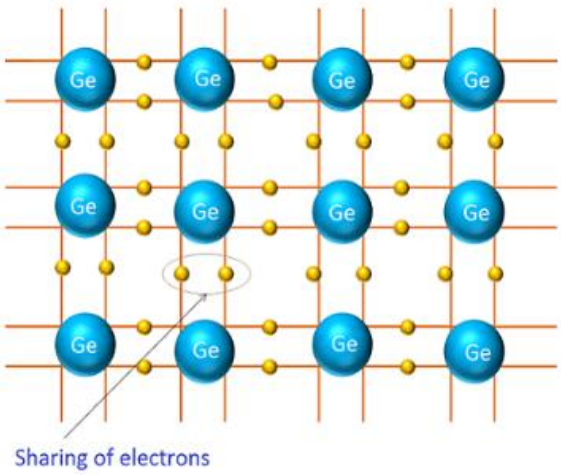

Figure 15: The sharing of electrons for the germanium atom

The second category of semiconductors is with dopants, if there is an endogenous semiconductor, such as germanium (Ge), is added a small quantity of element with oxidation state 5^+, such as arsenic (As), the 4 valance electrons of As will be create with the 4 corresponding atoms of the neighboring atoms Ge covalent bonds and will remain unbound the fifth electron of the atom As, which can easily be removed due to thermal movement, even at low temperature, as shown in the next figure. The atom of arsenic called donor.

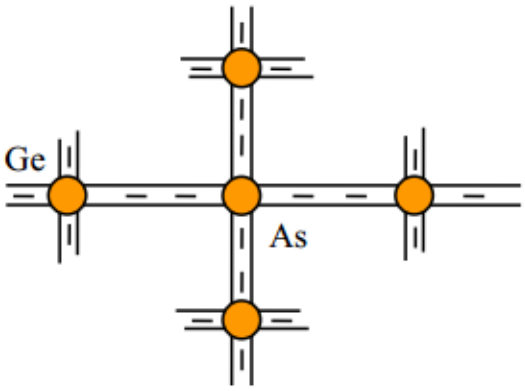

Figure 16: Schematic depiction of n-type semiconductor

Increasing the number of donors in semiconductor Ge, increases the number of free electrons with the result of creating a small current when the semiconductor found in electric field. This type of semiconductors called ***n-type*** semiconductor. If an element with oxidation state 3^+, such as gallium (Ga) inserted into a semiconductor Si, then the 3 valance electrons of Ga create covalent bonds with the 3 valance electrons of neighboring atoms Si, while this does not with the fourth neighboring atom of Si, which appears in following figure.

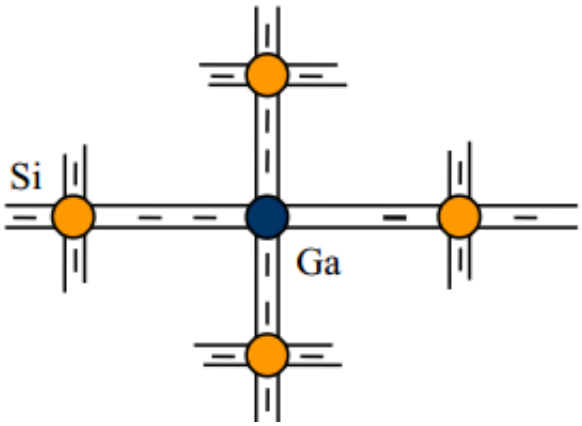

Figure 17: Schematic depiction of p-type semiconductor

The position of the missing electron to complete the covalent bond is a hole in the crystal lattice and may be covered by a valance electron of a neighboring atom Si, which will move to that position. The dopants of which the atoms attach holes in crystal lattice and thus accept electrons called acceptor or ***p-type*** semiconductor. Of this type semiconductor the number of holes is much larger than that of an endogenous semiconductor.

4. The characteristics of the photovoltaics devices

4.1 Equivalent circuit

A macroscopic equivalent circuit includes the following:

- ✓ ***A current source***, which represents the photocurrent produced inside the cell. This current moves in opposite direction from the correct polarization of a diode and depends on the voltage at the ends of the device.
- ✓ ***A voltage source***, which in the ideal case, is an element of circuits maintaining a certain voltage at the terminals independently of current flow in those terminals. This voltage may be continuous or alternating with time.
- ✓ ***A resistance of series (R_s)***, which collects the behavior of the electrode as well as the contact between the organic semiconductor and the metal. It has shown the ability of the organic material to allow the mobility of charge carriers. It is usually reduced by reducing the thickness, increasing the temperature and increasing the intensity of light.
- ✓ ***A shunt resistance (R_{sh})*** that gives the power of the current flowing through the device, which reflects the overall quality of the active layer film. In contrast with R_s, the R_{sh} should be maximum to achieve the maximum performance of solar cell. It has been found to increase with the reduction in

thickness, while remaining stable with the increase in temperature and dramatically decreasing with the increase in the intensity of light.

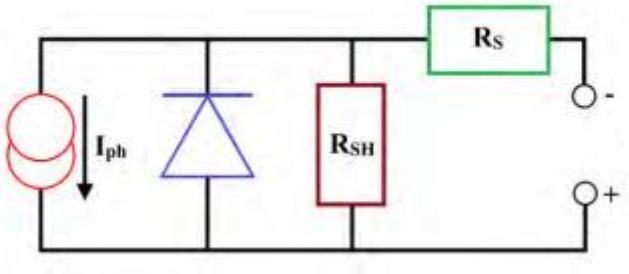

Figure 18: From left to right are distinguished: a current source, a diode, a shunt resistance Rsh, a resistance of series Rs and a voltage source.

4.2 The I-V characteristic curve of solar cell

The following graph shows the characteristics sizes current-voltage of a typical solar cell operating under normal conditions. The power produced by the solar cell is the product of the current and the voltage (I x V), for all the voltages from short-circuit to open-circuit conditions, where the curve is taken for a given radiation station. When the solar cell open-circuited, that is not connected to any load, the current will be at its minimum (zero) and the voltage across the cell is maximum, known as the open circuit voltage (V_{oc}) at the solar cell. From the other side, when the solar cell is short circuited, that is the positive and negative conductors connected together, the voltage across the cell is minimum (zero) but the current flowing out of the cell reaches the maximum, known as short circuit current (I_{sc}) at the solar cell.

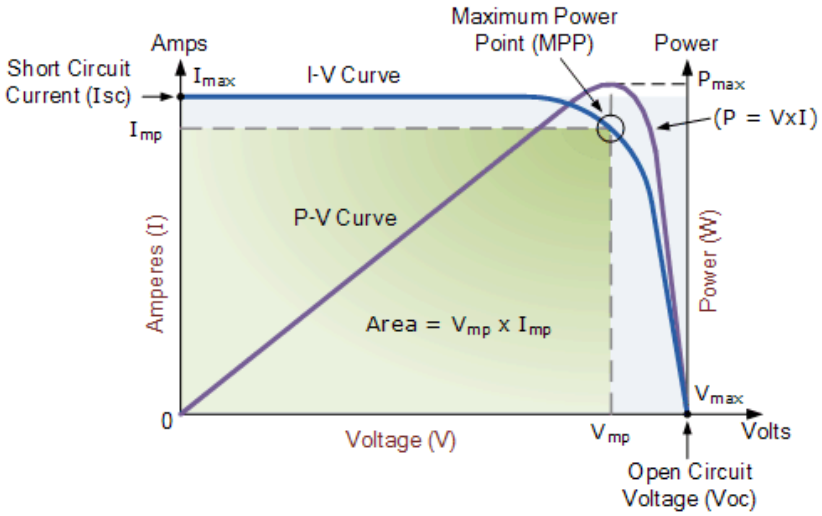

Figure 19: The characteristics curves (I-V) &(P-V) for solar cell

However, the curve of power-current (P-V) presented one particular combination of current and voltage for which the power reaches the maximum value, at I_{mp} and V_{mp}. In other words, the point at which the cell generates maximum electrical power and

this is shown at the top right area of the green rectangle. This is the "maximum power point" or M_{pp}. Therefore, the ideal operation of a solar cell is defined to be at the maximum power point. The maximum power for a solar cell which can give under a given radiation density is equal to $P_m = I_m * V_m$. The maximum power point (P_{MP}) of a solar cell is located near the point in the I-V characteristics curve. The specific values of V_{mp} and I_{mp} can be estimated from the open circuit voltage and the short circuit current: $V_{mp} \cong (0.8–0.90)\ V_{oc}$ and $I_{mp} \cong (0.85–0.95)\ I_{sc}$. Since solar cell output voltage and current both depend on temperature, the actual output power will vary with changes in ambient temperature.

4.3 Standard test conditions of characteristics of solar cells

The characteristics sizes which are tested in laboratory prepared photovoltaic modules as well as the available final product are: the energy efficiency (n), the fill factor (F.F.), the short-circuit current (I_{sc}) and the open-circuit voltage (V_{oc}), in specific lighting conditions (power density and the spectrum of the incident radiation) and the temperature of the photovoltaic. Consequently, to control the efficiency of solar cell it must be known the characteristics sizes under the specific conditions, representing typical conditions of exploitation of solar radiation. Thus, determined internationally, the following standard test conditions for controlling the characteristics of a photovoltaic cell or photovoltaic modules.

Standard Test Conditions (STC)

- The vertical impact of radiation on the face of the solar cell.
- The temperature of photovoltaic: $\theta_{STC} = 25^{\circ}C \pm 2^{\circ}C$.
- Electromagnetic radiation of parallel radiation beam, power density $E_{STC} = 1kW/m^2$ and the spectrum corresponding of solar with AM1.5.

In fact, the photovoltaic elements incorporated in the unit called photovoltaic panel, which operate under the natural sunlight whose characteristics change over the course of the year. Finally, based on standard conditions, the concept of peak power P_p is introduced, as a feature of photovoltaic, with unit in SI the Peak Watt ($W_{p)}$, which is the maximum electrical power that can yield below the standard control conditions. (STP, $P_p = P_{m,\ STC)}$

4.4 The individual characteristics sizes

1.Open circuit voltage (V_{oc}): is the maximum voltage that the cell provides when the terminal isn't connected to any load (an open circuit condition). This value is much higher than V_{mp} which relates to the operation of the photovoltaic which is fixed by the load. This value is dependent on the number of photovoltaics panels connected together in series.

2.Short circuit current (I_{sc}): is the maximum current provided by solar cell when the output connectors are shorted together (a short circuit condition). This value is much higher than I_{mp} which related to the normal operating circuit current. Generally, the electrical current produced in a photovoltaic reactor indicates the number of photo

generated carries which end up collected on the electrodes. This ratio for current is related in other three factors which are noteworthy be analyzed.

1. ***The absorption efficiency of the active material (n_{abs}):*** this value depends on the absorption spectrum of the active material, as well is also associated with interference effects taking place within the structure of the active material film. the absorption spectrum of the active material should be the same and with the spectrum of solar radiation, but that is not always the case possible, since most organic materials have a fairly narrow absorption spectrum and with a maximum usually less than the maximum of the solar spectrum (~ 800 nm). In general, the organic photovoltaics or perovskite solar cells include a transparent substrate until the radiation reaches the active material, with the result reducing the intensity of incoming radiation. On the other hand, the metal electrode exhibits intense reflection and contribute to increasing absorption. Therefore, both reinforcing as well destructive optical interference occurs within the organic photovoltaic suggesting the need to normalize both the thickness of the active layer and the cooperation of all the interlayers with each other, in order to maximize the absorption of the photons.
2. ***The efficiency of the disintegration of excitons (n_{diis}):*** is the value which depended on the effectiveness of materials to disperse created excitons, where, the efficient disintegration of excitons requires the optimization of the interface between the active layer and the other layers.
3. ***The collection efficiency of the free carriers from electrodes (n_{out})***: the electrons and holes will have to find continuum roads to reach the respective electrodes. However, the value of the n_{out} severely limited by the low mobility of charge carriers which have the organic semiconductors. The mobility seems to increase with increasing temperature and the imposition of an external electric field, following a relationship of *Poole-Frenkel* form, as shown in the equation below: $\mu(E)= \mu_o * e^{\gamma\sqrt{E}}$, where factors γ and μ_o depend on temperature, μ_o is their mobility carriers without the application of electric field, the short-circuit current usually increases with the temperature increase due to the dependence of the mobility of the charge carriers on it.

Consequently, the short circuit current is analogous from these factors and is symbolized as $I_{sc} \propto n_{out} * n_{diis} * n_{abs}$.

3.The efficiency of solar cells (n): the factor that gives the overall picture of a solar cell is the overall power conversion efficiency of the cell and defines by the following type, $\mathbf{n= (V_{oc} * J_{sc} * FF) / P_{in}}$ and usually calculated as the percentage of a hundred, where in the above equation **n** is a power conversion efficiency (PCE), $\mathbf{V_{oc}}$ is open-circuit voltage (when the I=0), $\mathbf{J_{sc}}$ is the short-circuit current density (when the V=0) and P_{in} is the power of the incoming radiation, which is usually normalized to $100 mW/cm^2$ (AM1.5).

4.Fill factor (F.F.): is given by the quotient of maximum power and the product of the open circuit voltage with the short-circuit current density and equals with: **FF= (J_{mp}*V_{mp})/ (J_{sc}*V_{oc})** and usually calculate as the percentage of a hundred.

5.External Quantum Efficiency (EQE) or Incident Photon to Current Efficiency (IPCE): is a measurement which show us the number of carries which collected by solar cell to the number of photons of an incident given energy on the solar cell. The quantum efficiency may be given either as a function of energy or wavelength. They appeared two types of quantum efficiency: 1) External Quantum Efficiency (EQE) and 2) Internal Quantum Efficiency (IQE).

1. **External Quantum Efficiency (EQE):** is the rate between the number of the collected carriers and the number of all the incident photons from the active area on the device at a given wavelength.
2. **Internal Quantum Efficiency (IQE):** is the rate between the number of the collected carriers and the number of all the absorbed photons by only the active absorber at a given wavelength.

The principle of EQE measurement is based on illuminating the sample by a monochromatic light and recording the device electrical current (number of generated carriers). By varying the frequency of the light the entire curve of the current as a function of wavelength can then be established. In following figure, shows an example of EQE curve for a typical silicon based solar device. The area under the curve will then represent the total number of carriers created by the device under full spectrum white light illumination. In other words, the integration of the curve will give the electrical current density.

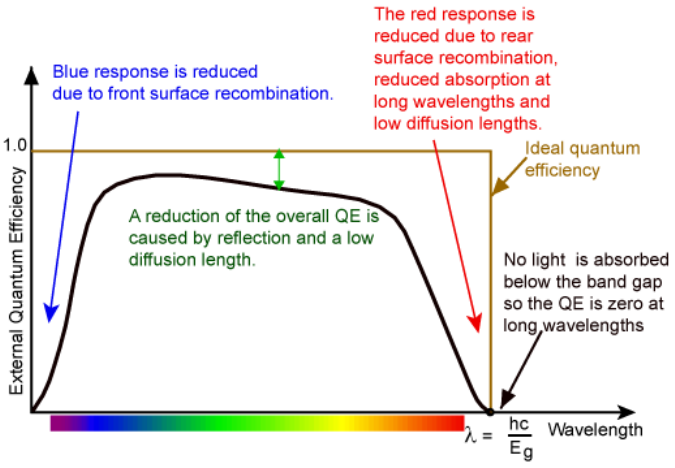

Figure 20: A typical External Quantum Efficiency curve of a silicon solar device

In order to determine IQE the light absorbed by the active layer stack has to be identified. This is typically done by recording and excluding the light reflected from the device and using only the absorbed portion of light for the calculation of quantum efficiency. Since the absorbed light is typically less than the total incident light (as there will always be some loss of light due to reflections) then

EQE will typically be less than IQE. The difference between IQE and EQE is important for distinguishing loss mechanisms between optical absorption properties of the entire device and photo conversion properties of the absorbing materials. IPCE is also useful for studying degradation properties of devices. The general reduction in the IPCE during time points to deterioration of photo conversion properties of the active material, while the change of the shape of the IPCE curve may point to morphological alterations in the absorbing layer.

4.4 The structure of solar cells

For the manufacture of solar cells have been mainly reported 3 typical structures depending on the energy levels and the properties of perovskite layer and other materials used in the other layers. These 4 categories are: a) mesoporous (n-i-p) structure, b) mesoporous (p-i-n) structure c) conversional (n-i-p) planar structure, d) inverted (p-i-n) planar structure and presents the following picture.

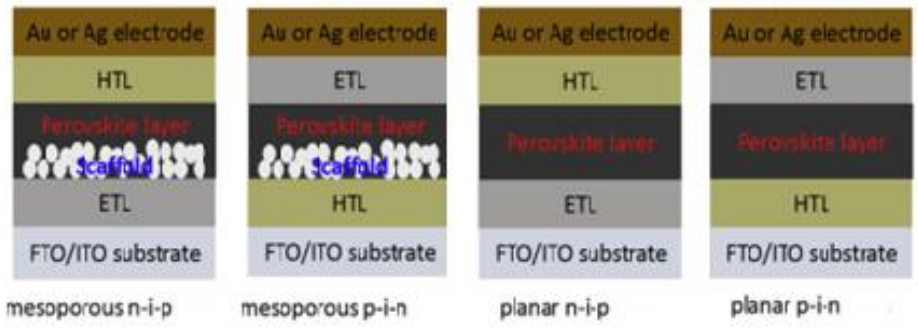

Figure 21: The 4 typical structures of perovskite solar cells

The operation of these structures, for example, in the inverted planar structure, a hole transporting layer (HTL) is deposited or sometimes on the transparent conductive oxide (TCO) substrate mostly indium tin oxide (ITO) and more rarely the fluorine doped tin oxide (FTO) as cathode, then the perovskite materials deposited with spin coating and after this, deposited an electron transporting layer (ETL) and metal electrode, mainly Ag or Al as anode.

Hole transport materials: There are 3 significant categories of materials which are used for hole transport layer. Regarding these are 1) inorganic, 2) organic small molecule and 3) polymer materials.

Their main function is to collect and transporting the holes to the corresponding electrode from the light harvester with the aim of achieving the proper separation of holes and electrons. Also the other features they need to have are:

1. High mobility of holes
2. Photochemical stability

3. The highest occupied molecular orbital (HOMO) is matched with valance band (VB) of perovskite material, therefore successful hole transport
4. To be soluble in organic solvents to form a good film for further manufacture and processing of device.
5. Appropriate light absorption in visible and near-IR area of the solar spectrum for high photocurrent.

The important materials used for hole transport are summarized in next figure

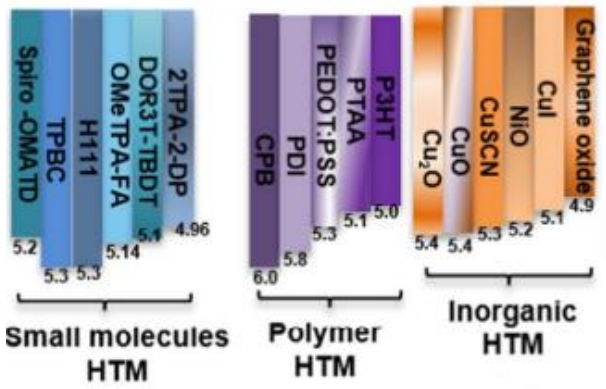

Figure 22: The most useful materials with the (HUMO) level for hole transport layer in solar cells

For example, one of the most useful material from the polymer category is the PEDOT: PSS. It usually uses in inverted planar structure in solar cells, it being processed at low temperature <100˚C and that it does useful for flexible substrate. It's transparent, it has good properties for film forming and the work function is high (~5.3eV). From the category of the inorganic material, the most wanted material is nickel oxide (NiO). It has good conductivity of holes, the valance band matches with valance band (5.2-5.4eV) of perovskite material, has large energy gap but it has high processing temperatures.

All of these materials play an important role for the fabrication of the device and will depend on the efficiency and characteristics size. Therefore, the photocurrent is determined by the rate extraction of holes and electrons. The fill factor is improved with the improvement from the hole mobility and the conductivity from these hole transport materials. Finally, for the open circuit voltage will obtain high charge mobility as well as suitable energy level alignment.

Electron transport materials: The most common materials for use on electron transport layer (ETL) are: 1) $PC_{60}BM$, 2) T_iO_2, 3) ZnO, 4) SnO_2, proportionally with the energy levels and the structure chosen to construct the device is taking place.

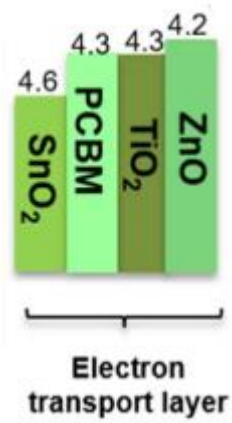

Figure 23: The most useful materials with the (LUMO) level for electron transport layer in solar cells

The main conditions that these materials must meet are:

1. Electrical properties: they should have a lower highest occupied molecular orbital (HOMO) than of the perovskite material, in order to accept electrons and at the same time block the holes and to prevent the carrier recombination by reducing the material structural disorder. Also a high conductivity with the electron mobility higher than perovskite layer to exclude any charge accumulation at the interface that can result the degradation of the device.
2. Film morphology: Due to the ambipolar transport property of perovskite material, a pinhole-free dense morphology of the ETL is important for highly efficient devices, because the current leakage from pinholes in the film and the charge recombination at the electrode interface can be avoided to obtain a high shunt resistance.
3. Hydrophobicity and chemical stability: For an efficient electron transport layer can't exist the moisture because will react with perovskite materials and lead to degradation of the device and the chemical stability play an important role, to avoid chemical reaction with the cathode electrode and perovskite layer.

For example, all these materials that have already been used have many advantages and disadvantages for the use in electron transport layer. Firstly, the T_iO_2 it has large bandgap, the conduction band is slightly lower than the perovskite material, so it can be successful electron injection from the perovskite absorber to electron transport layer through direct contact and it has blocked the holes. But it has and disadvantages which can decreasing the efficiency and the stability of solar cells. The most of them are: the low conductivity, the high processing temperature and the high density of trap states. Another material is from the category of fullerene derivatives which is successful the choice for the electron transport material is $PC_{60}BM$. This material has the ability to exhibit minimum or negligible current hysteresis, which has been regarded as the result of the trap-passivation and ion-migration-blocking functions of fullerene on the perovskite surface and in grain boundaries, combined with the fast

charge transfer from the perovskite to the fullerene in the electron transport layer (ETL). The difference between $PC_{60}BM$ and PCMB is that the $PC_{60}BM$ can be packed more densely than PCBM to facilitate intermolecular charge transport and shows much higher electron mobility and conductivity compared to PCBM. In the next picture there is a structure of a device that shows the effect of this material on the site of electron transport layer.

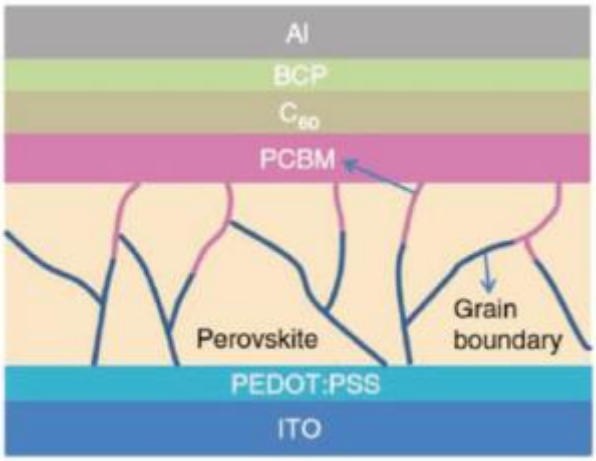

Figure 24: The diffusion of fullerene into the grain boundaries of perovskite thus passivating trap states

Two factors affecting positively the choice this material, $PC_{60}BM$ for electron transport layer and it seems the positive effect on the characteristics sizes for the device is the temperature for the annealing of fabricated structure and the passing of time from the deposition of the material, whereby covering the imperfections of the active layer is achieved and consequently results in the structure of a uniform film and interfaces excluding the hysteresis and the charge recombination.

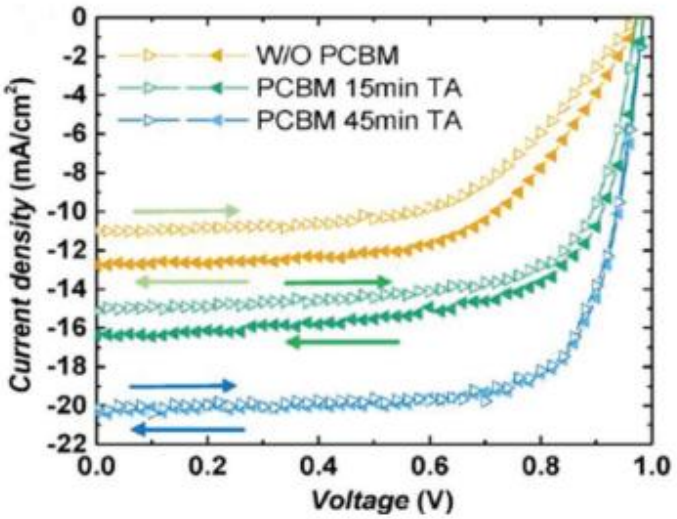

Figure 25: J-V curves for perovskite solar cells with thermal annealing of the PCBM layer

4.5 The role of intermediate layers

The introduction of intermediate layers into the perovskite solar cells, either the anode electrode and the active layer either the active layer and the cathode electrode has led to a significant improvement in the performance of the photovoltaic characteristics. The materials that used in such applications will have to obey certain basic requirements to be able to perform their role as hole transport layer (HTL) and electron transport layer (ETL):

1. These materials should have the ability to collect only their carries of the desired charge and repel the others, in the HTL, that is to say, the collection of holes and the electrons are suppressed, while the ETL should be the opposite, that is to say the collection of electrons and the holes are suppressed.

2. The materials for such applications should be stable and not increase the resistance in series of the device.

3. These materials should have a low absorption of light, especially when its layout device is such that the HTL or ETL is interposed between the transparent electrode and active layer.

4. They should be able to transfer the carries that they collect to the respective electrodes with high efficiency, for example, the holes will have to be transferred via the HTL to anode and electrons through the ETL at the cathode.

In general, we can say that a material used as HTL should provide the necessary alignment of energy levels between the active layer and of the anode electrode and will improve the collection of holes from this electrode. One material used as an ETL, should accordingly provide the necessary alignment of the energy levels of the active layer and the cathode electrode and, at the same time, to improve the collection of electrons from the cathode.

5. Experimental

5.1 Equipment

The equipment that was used for the fabrication of a solar cell is referred bellow.

- **Sonicator**
  Ultra-sonication is required for cleaning of the substrates. In this process sound energy is applied (200-400 kHz) to a container where a solvent and the substrates are placed. The solvent is usually water. This phenomenon creates rapid vibrations around the substrates that remove most of the contaminants such as dust, dirt (etc). In this work Elma Sonicator by Elmasonic was used.

Figure 26: Sonication System by Elmasonic

- **Uv ozone**
  Ultraviolet ozone treatment is a subsequent method of cleaning the substrates. The specific method aims to remove the organic contamination and increase the surface hydrophilicity in order to deposit a uniform layer afterwards. This effect is caused by irradiating the surface of a substrate with suitable lamps that emit ultraviolet light at wavelengths of 185 nm and 254 nm. It is a photo-sensitized oxidation process by atomized oxygen and high reactive ozone. The UV ozone cleaner that was used is a MB-UV-O3-Cleaner by MBRAUN.

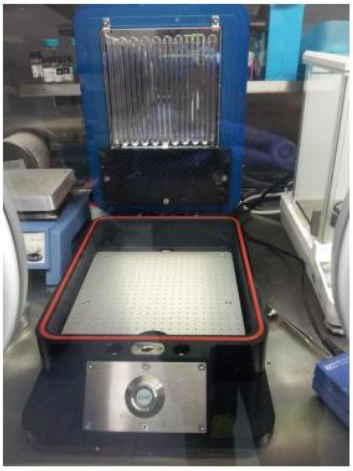

Figure 27: The UV-ozone cleaner system in glovebox

- **Vacuum filtration**
  The vacuum filtration is a fast filtration technique which is used to separate solids from liquid materials. The experimental setup includes a glass funnel that contains the solution which is then filtered by vacuum, so that the material of interest stays in the membrane and the solvent is removed. The device that was used was bought from the company Millipore Corporation.

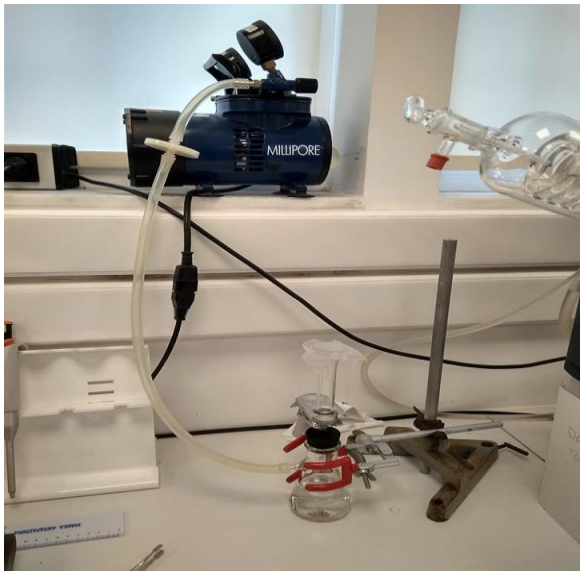

Figure 28: The vacuum filtration and the pump system that was used.

- **Spin coater**
  The process wherein the deposition material to create a uniform thin film on a flat substrate is made by spin coating. The rotation of a substrate at specific speed means that the centripetal force combined with the surface tension of the solutions of the solution pulls the liquid coating into an even covering. The solvent during the spin coating evaporates so as to leave a material in a uniform film on the substrate. Two spin coaters were used for deposition of materials, was found in glovebox, the first spin coater was used for the deposition of perovskite materials and the second spin coater was used to deposit the others materials for HTL or ETL.

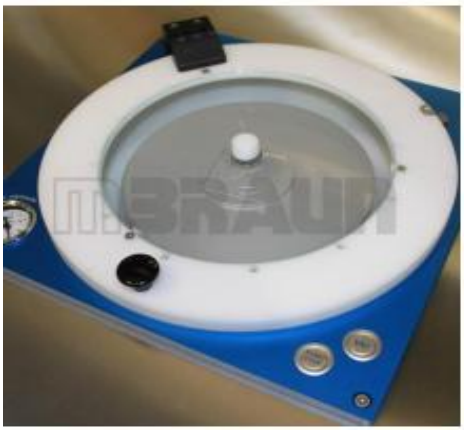

Figure 29: The spin coater MB-SC-200 by Ossila for the deposition materials for HTL or ETL

Figure 30: The spin coater by Ossila was used for deposition of perovskite materials

- **Glove box**
  Glove box is a sealed container that is designed to allow one to manipulate objects where a separate atmosphere is desired. Typically, a glove box is filled with nitrogen, an inert gas which is used to avoid unwanted chemical reactions degrading a sample. Furthermore, the inert gas in a glove box is pumped through a series of treatment devices which remove solvents, water and oxygen from the gas. All of above make the glove box a high purity inert atmosphere container, suitable for manipulating sensitive to oxygen and water materials. A MB 200B Modular glove box work station was used by MBRAUN.

Figure31: The MB 200B glovebox system by MBRAUN

- **Evaporator**

  Thermal evaporation is method of thin film deposition. The solid material is heated in a high vacuum chamber, reaching a melting point temperature where it produces some vapor pressure. The vapor stream of the evaporated material traverses the chamber to reach the substrate and make a coating. The high vacuum is required so that the evaporated particles can travel directly to the substrate without colliding with the background gas. Once the particles reach the substrate, they condense back to solid state forming a compact thin film. The MB-EcoVap by MBRAUN evaporator system was used. In this work is used silver(Ag).

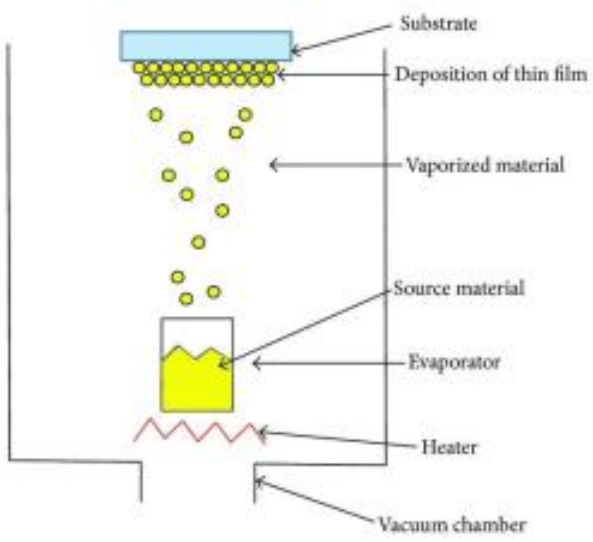

Figure 32: The evaporated particles travel to substrate

Figure 33: The MB-EcoVap evaporator under high vacuum (left) and with the vacuum chamber open(right).

- **Solar simulator**
  A solar simulator is a device that gives illumination similar with the natural sunlight. In our laboratory is located in glovebox and can be measured the devices after is located to the specific mask. The aim is to provide a controllable indoor test facility under laboratory conditions.

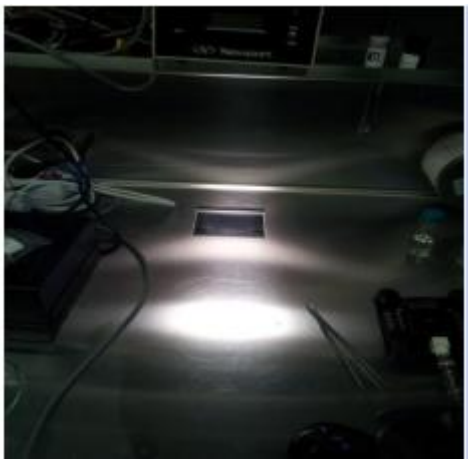

Figure 34: Solar simulator irradiating white light

5.2 The steps for preparation of perovskite solar cell

For the preparation of perovskite solar cell, it is necessary to analyze 5 important steps in order to have a successful device:

1. 4 steps cleaning of Anode-ITO substrate
2. Deposition of Hole Transport Layer- PTAA layer
3. Deposition of perovskite layer
4. Deposition of Electron Transport Layer- $PC_{60}BM$ layer
5. Deposition of Interlayer- PFN layer
6. Aluminum Cathode deposition

In general, it is desirable to fabricate perovskite solar cells in a cleanroom to produce results uniform and high-performance photovoltaics. Therefore, selected all depositions of materials be made within the glovebox. In order to avoid any dust and moisture in the atmospheric air because these materials are sensitive to these factors. Another important factor in fabrication the manipulation of substrates, where it should be only with tweezers and care must be taken to avoid touching the active area as this will scratch the films and cause failures due to shorting of the anode and cathode.

Figure 35: The tweezer for device safe handling

From the experiments were carried out the only material that needs to produce outside in glovebox is the PEDOT: PSS. The PEDOT: PSS has hygroscopic behavior and it has the strain to absorb easily water from atmosphere, so it is imperative the deposition and the annealing layer for this material be done outside from glovebox, to not affect the materials of the remaining layers consequently not lead to degradation of the device. It is also important the substrates to be clear and the right side, which is located the ITO substrate, which is found by the using of multimeter because the ITO layer is not visible to the naked eye.

5.2.1 Substrate cleaning process

As it was above referred, we have 4 step cleaning process followed for the ITO substrates. Firstly, we insert the substrates into a holder with the same direction and then immersion of them into a beaker with soap deionized water, as it seen in next Figure, after this step followed ultrasonic bath for 10 minutes.

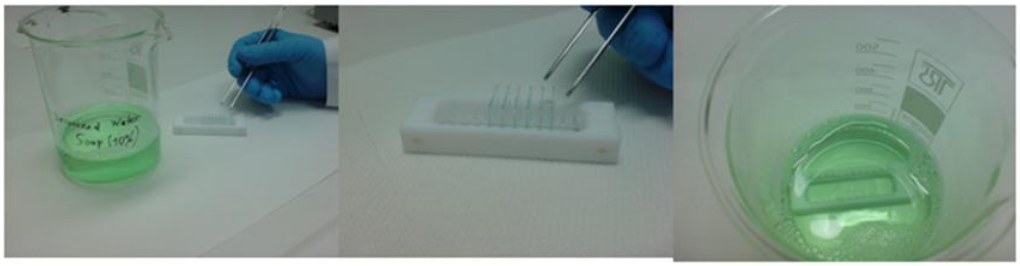

Figure 36: The first step preparation for substrate cleaning process

Figure 37: The ultrasonic bath

Next, followed rinsing the substrates with deionized water in order to remove the soap from the substrate. Afterward, is done the second immersion in acetone and the again the ultrasonic bath for 10 min. Finally, the third step is to rinse substrate with isopropanol (2-propanol, IPA) and then to immerse them in beaker with IPA, which followed ultrasonic sonication for 10 min, again. Then, substrates are transferred from the holder to the petri-dish with the ITO substrate side upwards and then placed in oven 120^{o}C for 15 min for drying.

Figure 38: The substrates are placed to a holder for drying

The last step is the placement of the substrates inside a vacuum UV-ozone cleaner chamber was done for 15 min at ~1 mW/cm^2 in order to remove any impure by atmospheric air and to increase the hydrophilicity of the substrate.

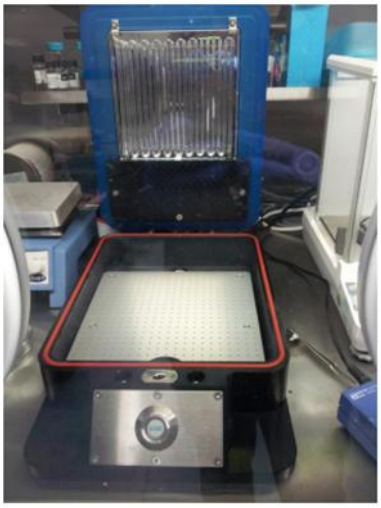

Figure 39: The UV-ozone cleaner system into the glovebox

5.3 Deposition of layers of solar cell

5.3.1 Positive electrode/Anode

For electrodes usually are used the transparent conducting oxides (TCOs) because they have unique optical and electrical properties. The main characteristics which must have a transparent conducting oxide are:

- High electrical conductivity
- High transparency in the visible range
- Superior stability

The most popular commercial transparent conducting oxide (TCO) is an Indium Tin Oxide (ITO). In our case, the glass substrates coated with ITO were purchased by Luminescence Technology Corp. Their dimensions are 20x15x1.1mm and the ITO layer has about 100nm thickness and a surface resistance of ~20Ω/sq. The energy level of ITO is ~ 4.7eV.

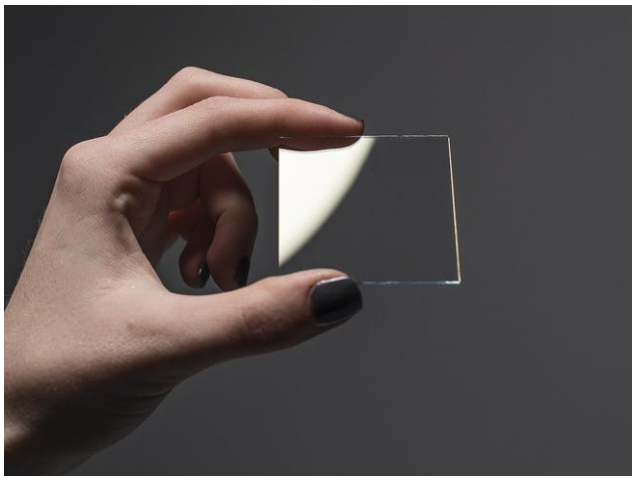

Figure 40: The glass substrate coated with ITO

5.3.2 Hole transport layer

In our case, for practicing fabrication solar cells has been chosen the inverted structure where significantly dependent from the energy levels of materials used. For hole transport layer was chosen a material which collected the holes and transfer to electrode and blocked the electrons in this place. The PTAA, (Poly[bis(4-phenyl) (2,4,6-trimethylphenyl) amine) is an excellent hole transporting and electron blocking semiconducting material due to its electron-rich components. The use of PTAA has been adopted that improve the open circuit voltage (V_{oc}) and Fill Factor (FF) of solar cells. In perovskite solar cells, the use of these hole transport material, improving all the characteristics sizes for solar cell. For example, J_{sc} of 16.5 mA/cm^2, V_{oc} of 0.997 V, fill factor of 0.727 and power conversion efficiency of solar cell more than 18% under standard illumination of 100 million watts/cm^2. These elements make the PTAA the best polymer material for hole transport layer of perovskite solar cells.

The solution of PTAA was prepared in a concentration 10mg/ml toluene where is stirred throughout the of our experiments. The deposition took place in glovebox with static spin coating at 4000rpm for 30 second and after that followed the annealing for 10 minute over hotplate to remove the solvent and to create a uniform layer. The work function of this material is 5.1-5.2 eV, is an important parameter chosen by specific material, because it has smaller than perovskite material and bigger than ITO substrate with work function 4.8 eV, so that it can charge collection, transfer holes to electrode and block the electrons in this place.

5.3.2 Perovskite layer (active layer)

For the fabrication of solar cells followed two step deposition perovskite layer. The solution of PbI_2 was prepared in concentration 450mg/ml DMF under stirring and heating overnight. The precursor of MAI was at concentration 45mg/ml anhydrous isopropanol under stirring overnight, until become the deposition. The dynamic spin coating done at 5000rpm for the PbI_2 layer for 40 second and the thermal annealing at 100˚C for 10 min at the hotplate. The MAI layer was deposited by dynamic spin coating at 5000rpm for 40 second and the thermal annealing was done at 100˚C for 1 hour. The CB of perovskite material is 3.9eV and VB is 5.4eV.

5.3.3 Electron transport layer

The $PC_{60}BM$ is the most usual material that used for collection and transport of electrons from active layer to cathode electrode. The HOMO level is 6.1 eV and LUMO level is 3.7 eV that matched exactly with band alignment to perovskite material, it has the property with the deposition to cover the defects of perovskite layer. It has a high electron mobility and helps to have efficient charge transfer and exciton dissociation. The solution of $PC_{60}BM$ was prepared in concentration 20mg/ml chlorobenzene anhydrous to 70˚C and stirring overnight. The dynamic spin coating done at 1000rpm for 45 second and the annealing was done in the glovebox to the room temperature order not to affect the perovskite layer.

5.3.4 Interlayer

PFN is a conjugated polyelectrolyte used interlayer between ETL and cathode electrode. It is preferable for the cathode interface to have a low work function contact for efficient electron extraction and collection. While Al and Ag are the most common electrode materials, the thermal evaporation process frequently alters the quality of the metal/organic interface. The reactive hot metal atoms can lead to chemical interaction at the interface and diffusion into the organic layer. The PFN solution was prepared 0.4mg/ml methanol and 0.3 µl acetic acid where is stirred overnight. The deposition of PFN was done after half an hour from the deposition of $PC_{60}BM$ material at 2000rpm for 45 second with dynamic spin coating.

After all of these coatings for each individual layer is done the cleaning of material at the edges of the substrate, with the help of cotton wool and less solvent of each material, to avoid the risk of a short circuit and prevent recombination between electron transport and hole transport layers.

5.3.5 Negative (top) electrode/Cathode

The most common metal materials which were used for cathode are the silver (Ag) and Al (aluminum). The thickness of these materials was about 100nm. In this electrode is collected of the electrons from perovskite layer with the help of electron transport layer. The work function of Al is 4.2 eV and for Ag is 4.6 eV. The advantages of these materials have: i) long life, ii) high surface area per cathode, iii) low operating cost, iv) simple change the cathode area, v) easy replacement and vi) less heat buildup.

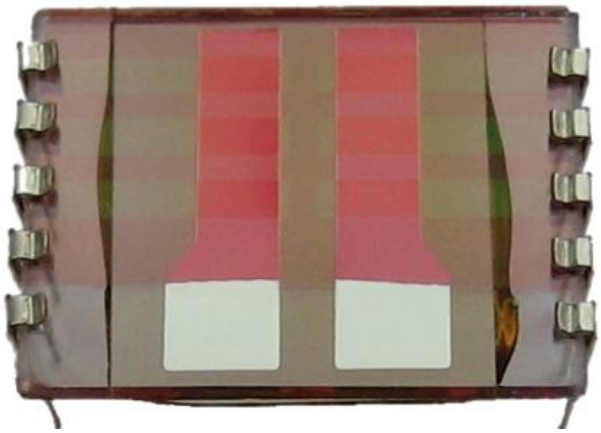

Figure 41: Aluminum cathodes in solar cells

5.3.6 Deposition of cathode/ negative (top) electrode by Thermal Vacuum Deposition method

One of the main physical vapor deposition method is Thermal Vacuum Evaporation. This is a form of thin films that are used with aim to become the coating of pure materials on the surface of various objects. These objects are referred as substrates and can be: solar cells, optical components and semiconductor wafers. The coatings made on the substrate can be a single material or multiple materials in layered structure and the thickness ranges from angstroms (Å) until microns (μm). The Thermal Vacuum Evaporation get started with the heating of a solid material inside high vacuum chamber until it reaches a temperature that produces some vapor pressure. Inside the vacuum, even a relatively low vapor pressure is sufficient to raise a vapor cloud inside the chamber. This material crosses the chamber and hits the substrate, sticking to it as a film or coating.

The material usually is liquid and is heated to the melting point, usually is located in the bottom of the chamber, often in some sort of upright crucible. The surfaces of substrates are properly inverted so as to make the coating of the heated material, while in appropriate fixtures at the top of the chamber. The evaporation system design gives us the opportunity can adapt various parameters, for example, the evaporation rate or the sensors for film thickness accuracy, to have desirable and regulated results such as the thickness, optical and electrical properties, the grain structure, uniformity, etc.

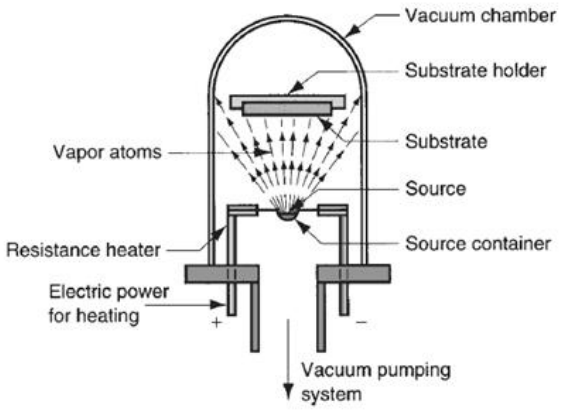

Figure 42: The set-up of vacuum evaporation

The coating of these materials can be made on specific parts of substrates with the use of shadow masks, leaving uncovered points you want to cover with material.

Figure 43: The placement of substrates in a cathode deposition mask

5.3.7 Table with the experimental characteristic values

In order to practice the fabrication of the perovskite solar cells, ***ITO/PTAA/PbI$_2$+ MAI/ PC$_{60}$BM/PFN/Ag*** solar cells were prepared. In the following table the measurements of the characteristic values for the fabricated devices are presented.

Table 1: Characteristic Values of experimentally fabricated devices

V_{oc}(V)	J_{sc}(mA/cm^2)	PCE(%)	FF(%)
0.994	22.16	11.18	54.38
0.993	22.57	11.28	53.66
1.019	22.26	11.35	52.52
1.007	17.49	11.46	65.03
1.025	18.39	11.73	64.41
0.979	20.09	11.76	60.04

1.01	20.31	11.79	56.12
0.98	20.76	11.81	60.12
1.002	19.06	11.82	63.54
1.014	18.21	11.83	63.8
0.996	20.76	11.89	57.47
0.998	21.003	11.91	56.8
0.993	19.94	12.1	64.96
1.003	20.11	12.14	64.49
1.008	20.21	12.15	59.64
0.998	19.70	12.16	61.77
1.004	19.97	12.22	61.06
0.989	22.18	12.39	58.64
1.006	20.95	12.53	59.44
1.007	20.32	12.99	63.48
1.008	20.32	13.09	63.81
1.021	21.5	13.26	60.45
1.039	21.7	13.27	58.83
1.022	21.29	13.28	61.01
1.016	20.99	13.33	62.48
1.028	21.91	13.37	60.47
1.024	21.42	13.38	60.94
1.02	21.22	13.41	61.95
1.021	21.3	13.48	61.99

6. Introduction of 2D materials

Two Dimensional materials are referred to as single layer materials, are crystalline consisting of a single layer of atoms. The 2D materials can be categorized as either 2D allotropes of various elements or compounds (consisting of two or more covalently bonding elements). In these materials, the electrons move free in the two-dimensional plane, as it happens to crystalline semiconducting materials, but their restricted motion in the third direction is governed by quantum mechanism. The thickness of these materials is few nanometers or less. These materials have used for many applications such as electrodes, photovoltaics, semiconductors and water purification. The elemental 2D materials generally carry the –ene suffix in their names while the compounds have –ane or –ide suffixes. Layered combinations of different 2D materials are generally called van der Waals heterostructures. The most

important materials which belong to the category of two dimensional materials are: boron nitrides, black phosphorous, transition metal dichalcogenides and the graphene. In this work will be given more development in the last two categories of materials mentioned above.

6.1 Graphene

Graphene is a planar allotrope form of carbon, wherein the carbon atoms form covalent bonds at one level. We can also consider it as the basic constituent unit from which all other allotropic forms of carbon are formed. Graphene is a rapidly ascending two-dimensional material (2D) with extremely high crystallinity and due to its unusual electronic properties, has already revealed new potential applications. Generally, graphene represents a new category of materials, thickness of a single carbon atom in hexagonal lattice, offering new inroads to the physics of small dimensions. The material was later rediscovered, isolated, and characterized in 2004 by Andre Geim and Konstantin Novoselov at the University of Manchester. The graphene corresponds to a monolayer of carbon sheet (2D) (taking its name from there) and is a key building elements for the construction of carbon-based nanomaterials. The graphene can be wrapped to form fullerenes (0D), to bend to form carbon nanotubes (1D), or finally to stack on graphite (3D).

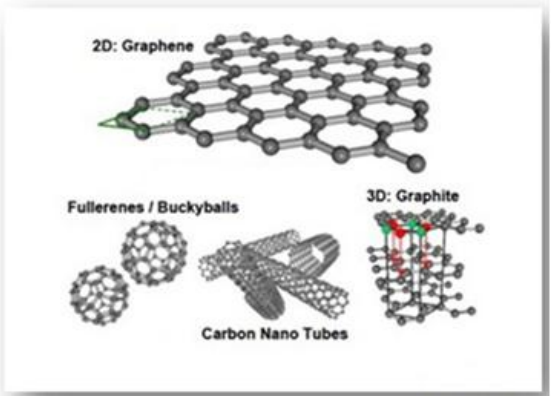

Figure 44: The various modifications of the graphene depending on the dimensions

The graphene is semiconductor with the bandgap to be zero, with high transfer and concentration capabilities and shows almost direct electron transfer at room temperature. It gives excellent electrical, thermal and mechanical properties that put it in front of other materials with regard to applications. It is also intended to be suitable for the construction of a new generation of flexible solar energy conversion devices and low cost optoelectronics devices, high-efficiency, thermal stability, low weight and environmentally friendly.

Several techniques have been developed for graphene production, each of which results in graphene with distinct properties. The main techniques developed for either isolation or graphene production are:

- ***Mechanical exfoliation of graphite***, is a technique by which it was confirmed the existence of graphene as a two-dimensional crystal by A. Geim and K. Novoselov 2004, and who were awarded the Nobel Prize in Physics in 2010. In this technique graphite sheets are isolated from the graphite by means of adhesive tape and then transferred to the desired substrate. Although from this technique the quality of the graphene produced is the best of all other techniques, however the disadvantage is to control the shape and quantity.

- ***The isolation of graphene in the liquid phase***, which occurs with the help of solvents and / or surfactants and the imposition of some external force in the process (ultrasonication, blender) improves the problem of the quantity produced, however, degrades its properties as it is difficult to remove the solvents and / or surfactants. This problem can be mitigated by the use of such materials, whose presence would not affect the application of graphene desired.

- ***The oxidation of graphite and the production of graphene oxide*** (GO) greatly increases the amount produced, however, the oxidized sheets of graphene although they become dispersed in many solvents, their remaining properties are dramatically reduced. The first method for producing GO was made by Hummer in 1958.

- ***The epitaxial growth of graphene*** on silicon carbide (SiC) substrates, is a technique that takes place under high vacuum and high temperature conditions, at which atoms of Si sublimate and bonds are formed between the carbon atoms. Although with this technique it is possible to check the number of layers and the size. However, the quality and energy requirements are the main disadvantages.

- ***The Chemical Vapor Deposition (CVD)*** is the technique synthesis of graphene in which control of size and quantity is best achieved, the quality although degraded relative to mechanical exfoliation, is in a good enough level to allow the application of the CVD graphene to several applications. In this technique, the development of graphene is done on metal surfaces (Cu, Ni) in high temperature conditions and atmosphere containing gas mixture (95% Ar and 5% H_2). To this mixture of gas also containing carbon rich materials (in gas phase), such as methane, which provide the necessary carbon deposited on the surface of the metal acting as a catalyst, and favors bond formation between carbon atoms.

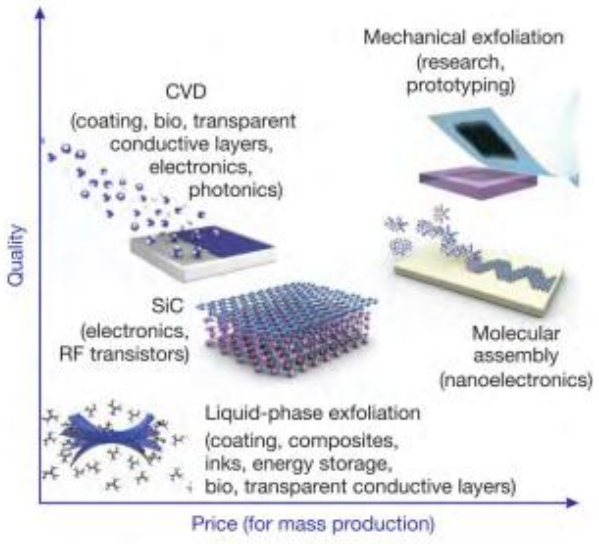

Figure 45: The several methods of mass production of graphene, which allow the choice of size, price and quantity for any particular application

Graphene oxide

Graphene oxide is easily modified, due to additional functionalities hydroxyl, epoxide and carboxyl groups, both on the surface and on the at edges, respectively. GO can be modified on both sides its surface and its periphery. The functional groups are identified on both sides by changing activity and allowing chemical bonds that would be unstable if only one surface was exposed. In some cases, this process can lead to unpaired electrons, which are generated at locations adjacent to the point of covalent bond, enhancing activity and leading to a reaction chain from the starting point of the attack. That's why the edges of GO are considered more active than the inner faces of the surface. The extra active sites, which usually facilitate graphene modification both on surface and on edges, are called imperfections. at the same time, imperfections are also called gaps created by excessive effort to create or isolation of a single sheet. The imperfections are mostly composed of oxidized carbon atoms at the ends in the form of carboxylic groups, hydroxyl groups, and on its main surface as hydroxyl and epoxy group. Finally, GO has interfacial strain, has good dispersion in water and is considered more hydrophilic. The presence of oxygen functional groups within at structure, such as the hydroxyl groups (-OH), the carboxyl groups (-COOH) and the epoxide groups -C-O-C-, reduce the forces that hold the graphite sheets together and give the graphene oxide a hydrophilic character. Thus, GO is soluble in polar solvents, forming stable suspensions.

For the production of graphene oxide is made by graphite oxidation. In the reactions for the production of GO, oxygen functional groups (carboxylate, hydroxyl and epoxy groups) are added to the sheets of GO at the base plane and its ends, respectively. The reaction of producing the graphene oxide from graphite, made using strong oxidizing agents ($KClO_3$, $NaNO_3$ or $KMnO_4$) as well as strong acids (H_2SO_4, HNO_3 or $HClO_4$). There are many methods of oxidation of graphite, such as De Brodie oxidation, Staudenmaier, and the most efficient modified Hummers method.

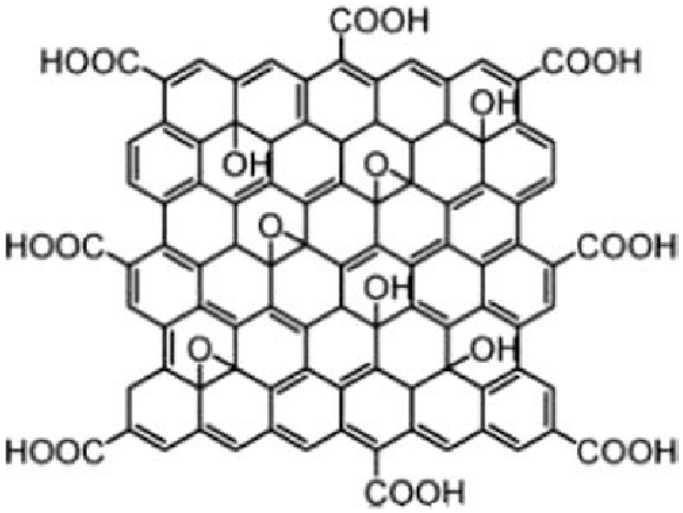

Figure 46: Structure of graphene oxide (GO)

Reduced graphene oxide (rGo)

GO is not conductive and therefore reduces the conductive form of reduced graphene oxide (rGO). The reduced graphene oxide is a material that retains all the exceptional properties of graphene and can dispersed in organic solvents resulting in homogeneous thin films. In particular, the oxygen present in the oxygen functional groups (-COOH, -OH, -O) are removed and replaced by hydrogens (H). The ways its reduction is: a) chemical, b) thermal and c) photochemical reduction. During the chemical reduction, GO is reduced by the use of chemical reducing agents, such as hydrazine, which is the most common reduction method.uring thermal reduction, oxygen functional groups are removed when GO is burned at a very high temperature (>900 °C). Finally, in the photochemical reduction using a laser, the bonds of the oxygen functional groups break and GO is reduced.he advantages of rGO are quite as it comes from carbon, so it is cheap and at the same time has great mechanical strength, elasticity, is permeable and electrically conductive. These advantages make this material ideal for future applications in optoelectronic devices.

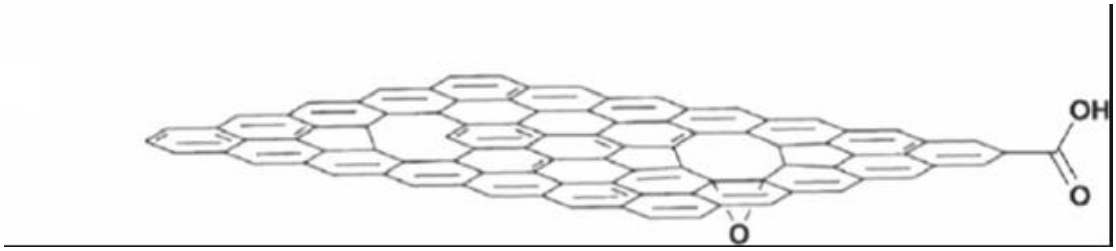

Figure 47: Structure of reduced Graphene Oxide

6.2 Graphene oxide as Hole Transport Layer in perovskite solar cells

In the research community, have been more successful structures of perovskite solar cells with GO as HTM. The improvement has observed at the characteristics sizes of solar cell. It has suitable work function (~4.9eV) which matched with the VB of the perovskite material with the result to be easier the charge transfers and the improvement of surface coverage. Also the use of GO can more effectively extracting the carriers from perovskite layer and reducing the carrier recombination because of the rapid carrier collection prevents charge accumulation at the interface of perovskite with the GO charge extraction layer. It is also can be found that, with increasing the GO thickness, the carrier extraction efficiency decreasing which might be caused by the poor conductivity of thicker GO layer. In the structure with composite GO/PEDOT: PSS has showed better characteristics sizes and efficiencies from simple structure with GO as HTM. The charge transfer became easier because the work function of this composite is between of GO (4.9eV) and PEDOT: PSS (5.1eV). Finally, the important improvement in long-term stability under the atmospheric conditions.

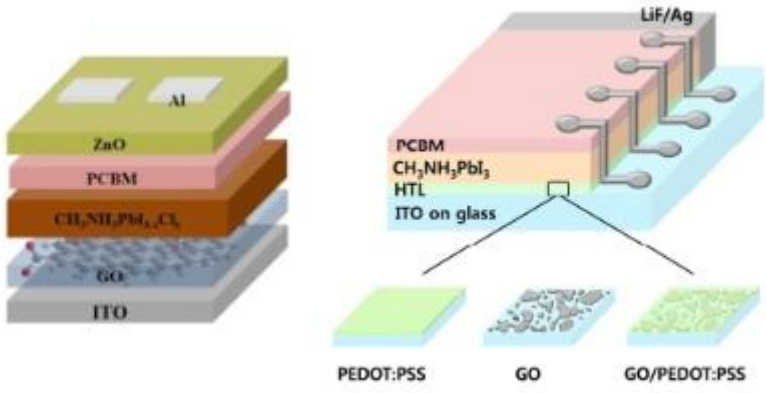

Figure 48: Structure of inverted perovskite solar cells with GO at HTM

6.3 Experimental course with Graphene Oxide for Hole transport layer

The aim of this experiment is to replace the material used for hole transport layer in the specific case the replacement of PTAA with GO, in order to see the effect on properties of the device and the influence on the characteristic values, consequently on the efficiency of solar cell.

6.3.1 Preparation of GO dispersion

First, the powder of graphene oxide that used, the laboratory has been supplied from GO supermarket for further processing and analysis of material. The properties of this material have been highlighted by the company. The color is dark grey, the flake size is 0.3-5 microns, the thickness is 1 atomic layer and the form is dry powder. They have previously weighed the vials that will introduce the powder so that it can be known and the concentration of the solution that produced. The material dispersed inside distilled water, followed 6 hours in bath sonication for better dispersion. After that, followed the centrifugation of solution at 2000rpm for 10 min, in order to allow precipitation of the material and obtain the supernatant for further use and through the sediment that will remain at the bottom of the container after drying to calculate the concentration of the final solution. In our case, produced solution with the next characteristics:

Table 1: Properties of GO dispersion

Initial mass of GO	Dispersion mass of GO	Solvent	Concentration
5.41 mg	3.36 mg	10 ml 2Dis H_2O	3.36mg/ml
5.05 mg	3.1 mg	10 ml 2Dis H_2O	3.1 mg/ml

Due to the low concentration of the solution with the dispersion of GO, it was chosen to become the deposition of material with the help at vacuum filtration and not with spin coating because wanted a uniform layer with material.

6.3.2 Deposition process steps with vacuum filtration of GO dispersion

To prepare the solution that is to be deposited on the membrane, 1ml from the solution of the dispersed GO was diluted further with 7ml of twice distilled H_2O in order for the GO to be more uniformly dispersed, followed by sonication in a water bath for 10 min. After that, the membrane is positioned as symmetrically as possible over the filter of the device. The membranes used were the MF-Millipore from Sigma-Aldrich. The properties of the membranes are:

- Hydrophilic and the color is white
- The pore size is 0.025μm
- 90mm diameter
- Mixed cellulose esters (MCE)
- The porosity is 72%
- The surface is plain

Figure 49: The mixed cellulose membranes that used for experimental procedure

After the solution of GO is ready to filter from vacuum filtration, a pressure adjustment is made to be low, to cover the material resources of the film and to form a uniform film gradually with time. The vacuum filtration should be stabilized so as to filter and form the film across the membrane uniformly. We cover the device of vacuum filtration with parafilm to avoid dust from the atmospheric air. All of solution penetrates from the membrane with the purpose to stay the material. The filtration time of the solution is 40-50 minutes, in order to avoid the risk of creating imperfections in the membrane and dry it well not to dissolve the film during immersion.

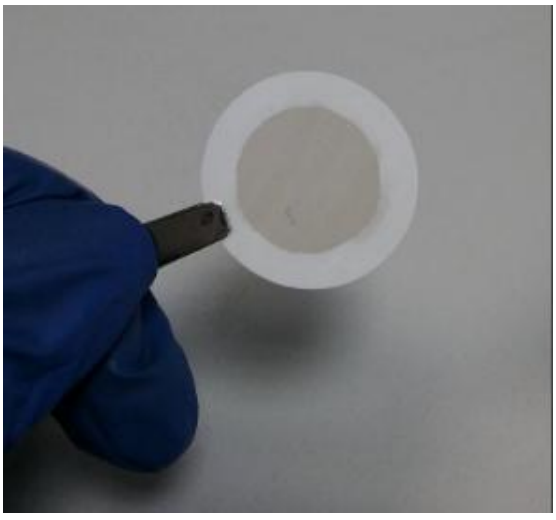

Figure 50: The membrane with GO for further use

Our substrates have been properly cleaned and the membrane cut to dimensions of substrate to make the pilling off.

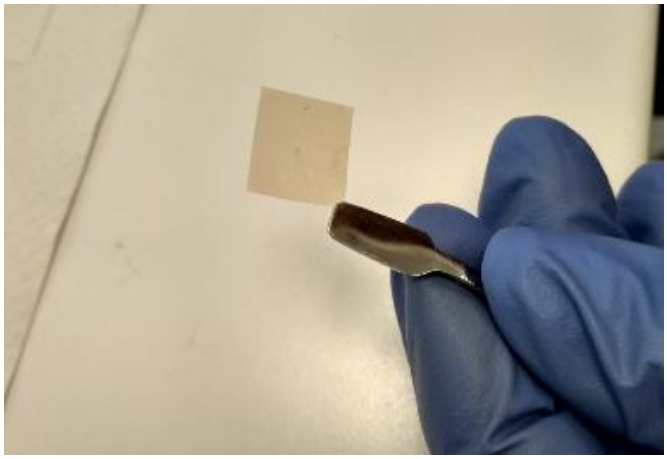

Figure 51: The membrane at dimensions of substrate

The dipping is done in double-distilled water for a few seconds, so you can make the transfer of the film to the substrate. We exert little force across the surface of the substrate to be successful the pilling off and placed a little piece of paper to absorb water immersion. Leave the membrane together with substrate overnight under a drags to a force of gravity. After this time as possible dipping again to leave the membrane and stay our material only and then gets annealing at 80˚C for 30 minutes.

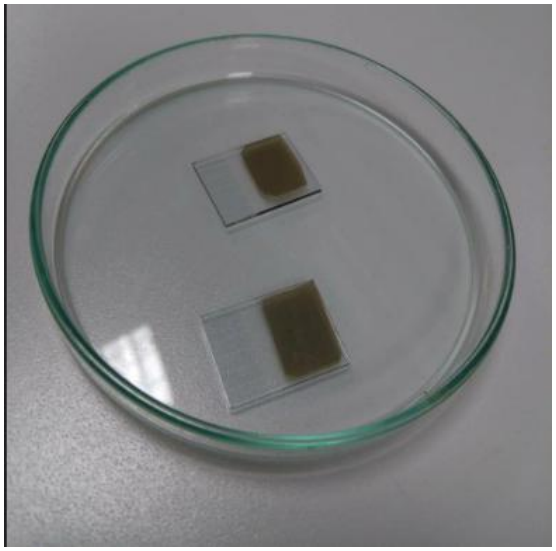

Figure 52: The deposition of GO after pilling off

To succeed to have a uniform film and permeability to have the right conditions for the replacement of hole transport material is done optimization of the thickness for GO films. Generally, the thickness and homogeneity of the GO films can be accurately controlled either by the concentration of the solution or by the volume of

vacuum filtration. The following table shows throughout the Experimental Procedures function of the volume of the solution took place with the help of Atomic Force Microscopy (AFM), the thickness of the layer was calculated and the film uniformity test was controlled.

Table 2: Experimental specific properties of GO material

Concentration of solution	***Thickness of layer***
1ml GO + 1ml 2dis. H_2O	~200 nm
1ml GO + 4ml 2dis. H_2O	313 nm
1ml GO + 8ml 2dis. H_2O	200-400 nm
1ml GO + 16ml 2dis. H_2O	134 nm
100μl GO + 1ml 2dis. H_2O	20-30 nm
100μl GO + 4ml 2dis. H_2O	~ 34 nm
100μl GO + 8ml 2dis. H_2O	15-100 nm
50μl GO + 1ml 2dis. H_2O	-
50μl GO + 4ml 2dis. H_2O	-
50μl GO + 8ml 2dis. H_2O	-

The last 3 concentrations that were processed could not be made to detach the film from the membrane and some in which the layer was achieved was not uniform. The most important factor for the continuation of the experiment was to be uniform but also a thin film. So the choice became in the film produced by concentration 100μl GO + 4ml 2distilled H_2O, with thickness at 34 nm.

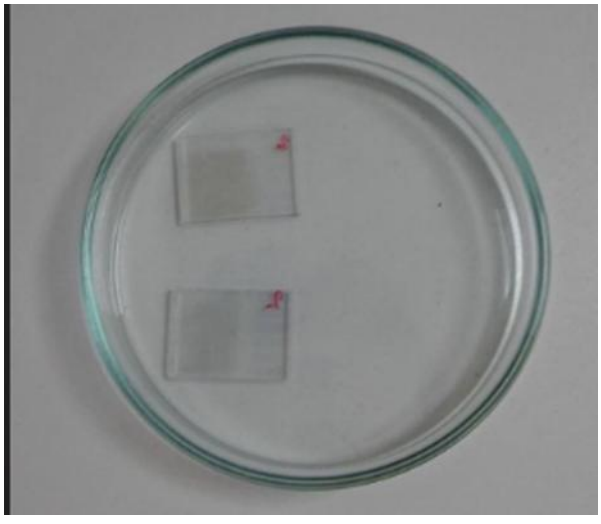

Figure 53: The most successful GO films with 34 nm thickness

The purpose of this experiment was the successful deposition of GO layer with the help of vacuum filtration, the optimization of the thickness of this layer so that it is permeable and at the same time homogeneous to be able to accept the remaining layers. The structure of the solar cell which have been selected to manufacture is: **ITO/GO/PbI_2+MAI/$PC_{60}BM$/Ag**.

The solution of this perovskite material is different from the perovskite that used at the first experimental solar cells. PbI_2 precursor in concentration 1.25M and MAI in concentration 1.25M added 300μl DMSO and 700μl GBL and stirring overnight. Also, the deposition of perovskite material was done in a different way. The deposition was done at 1 spin coating, but it has 3 steps. The first step is deposition the PbI_2 layer at 500 rpm for 5 seconds, the deposition of MAI at 2000rpm for 20 seconds and at the end 4000rpm for 20 seconds, where we cast the antisolvent, 300 μl toluene. at the initial stage during spin coating, the film is composed of MAI and PbI_2 dissolved in the DMSO/GBL solvent mixture, whereas in the intermediate stage, the composition of the film is concentrated by the evaporation of GBL. Then the toluene droplets lead to the immediate freezing of the constituents on spin coating via the quick removal of the excess DMSO solvent and the rapid formation of the MAI–PbI_2–DMSO phase, leaving a uniform and transparent thin film.

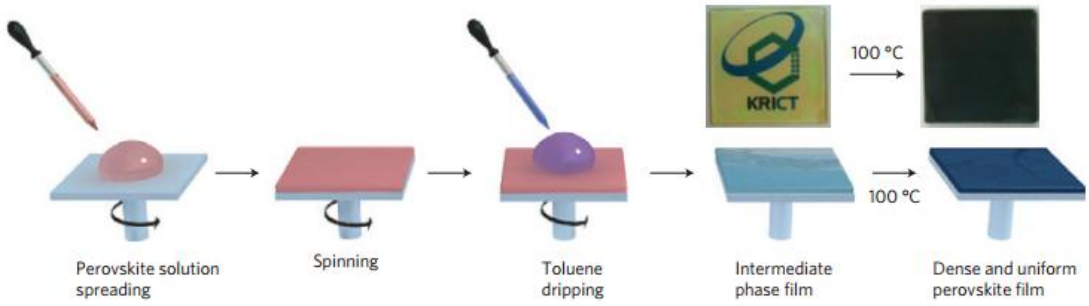

Figure 54: Solvent engineering procedure for preparing the uniform and dense perovskite film.

Then, became experimental testing with the best GO film at the thickness 34nm and with this perovskite material, in order to increase the conductivity of GO layer, with reduction. The concept was to done chemical reduction with reducing agent hydrazine for 1 hour into the glass container with the GO substrate, or with thermal reduction partly at 200˚C for 1 hour and photo chlorination with laser. Unfortunately, there have some technical problems with the high cost of membranes, the roughness of the surface that was big and the substrate has spikes and due to its no hydrophilicity, the placement of the perovskite layer could not be made. With the result, that the device for further electrical characterization cannot be created.

6.3.3 Characterization with UV- Visible Spectroscopy

The Ultraviolet visible spectroscopy is mainly used for the quantitative substance identification by correlating the percentage of absorption of electromagnetic radiation to the concentration of the substance responsible for absorption. When polychromatic radiation passes through a solution containing a substance, the power of the radiation decreases along the path due to absorption of the substance. Selective radiation absorption is performed because only the radiations whose photons have energies are absorbed correspond to the energy requirements of the molecule in order to stimulate it from a low energy state to a higher energy. Absorption in visible or ultraviolet radiation causes transients valence electrons. Each level of electronic energy contains many levels vibratory energy, each of which contains many rotational levels energy. It is possible to carry out, at the same time, many transitions electrons between power stations, which differ energetically between them a little bit. That is why the absorption spectrum in the visible and / or ultraviolet, which is due to electron stimulation, it is tapered and not linear. Interaction of materials with infrared radiation, causes vibrational changes in the molecules, higher energy (shorter wavelength) radiation in its area visible (400-700 nm) and ultraviolet (200-400 nm) causes individuals electronic transfers. Typically, absorption is associated with transitions induced in electrons of the bonded orbits, while the atoms involved in them are generally those containing electrons in the s and p individual orbitals. There are four types of electronic transitions that are can happen.

The following transitions may occur in one molecule:

- ✓ Transitions from n to σ* (e.g. oxygen, nitrogen, halogens, sulfur compounds)
- ✓ Transitions from n to π* (e.g. carbonyl groups)
- ✓ Transitions from σ to σ* (e.g. alkenes)
- ✓ Transitions from π to π* (e.g. carbonyl, alkenes, alkynes)

The transitions from σ to σ* and n to σ* require relatively high energy and therefore occur at very short wavelengths in the ultraviolet region, while the transitions from n to π* and from π to π* take place at lower energies, in the ultraviolet-visible region, as shown in the next figure.

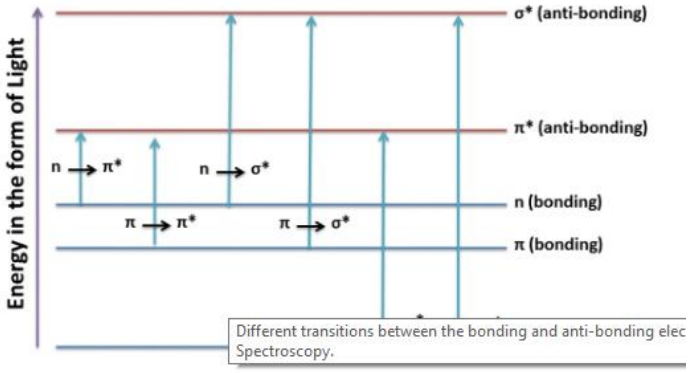

Figure 55: Four possible types of electron transitions

Since absorption spectrum contains information about electrons transitions, the starting point of absorption is considered as the optical energy a gap for materials such as semiconductors. The color that presents a molecule, in form solution or film, gives an indication of its energy gap. The color of a film or the solution perceived by an observer is usually complementary wavelength of the electromagnetic spectrum in which it absorbs the molecule. For example, if a molecule in a solution or film appears to be green, then the molecule absorbs the complementary color of the green, that is red color.

Instrumentation Spectrometry Ultraviolet – Visible

Absorption measurements are used for photometers and spectrophotometers. For the graphical depiction of absorption, A or T permeability in relation to wavelength λ is performed using a spectrophotometer. The basic units in an ultraviolet-visible spectrophotometer are below:

1. ***A radiation source***, of constant power, also referred to as a light source or just source. In the ultraviolet region a hydrogen or deuterium lamp is used, which along with continuous radiation (160-365nm) also emits linear radiation at longer wavelengths that can be used for adjusting the wavelength range of a monochromator. Its casing lamp consists of quartz or glass with a quartz window because the glass does not allow the passage of ultraviolet radiation.
2. ***Wavelength selector,*** to isolate the desired radiation. In quantitative spectrophotometric analysis is generally used wavelength range, because in this way selectivity increases sensitivity and concentration area. A wavelength selector may be either (optical) filter or monochromator (prism or diffraction barrier). Filters are cheaper wavelength selectors and there are many kinds of filters, interference filters and filters glass. Interference filters are those used in both ultraviolet and visible area. In the opposite case, those of the glass that their function is due to light interference phenomena. They consist of a thin layer of dielectric between semipermeable metal surfaces coated on glass tiles. Most commonly used is the monochromator with which exists possibility of continuously varying the wavelength during measurement. The main

characteristics are an entry slot from which the beam enters polychromatic radiation, a mirror with which the beam is made at the same time, a diffraction grating with a rotating selection the appropriate wavelength, a second mirror, and an exit slot which exits monochromatic radiation and whose range is playing an important role in the intensity of outgoing radiation

3. ***Cells,*** for sample placement. The material of construction of cell varies according to the area of the electromagnetic spectrum because it allows the passage of the corresponding radiation. So, use quartz for it ultraviolet (and visible) and glass for visible.
4. ***A detector,*** which converts the optical signal into an electrical signal, is usually one photomultiplier with short response time, lamp special construction high internal amplification emitting a large number of secondary electrons at the anode, and because of this the sensitivity of photomultiplier is particularly high.
5. ***A signal amplifier and a reading instrument***. (PC)

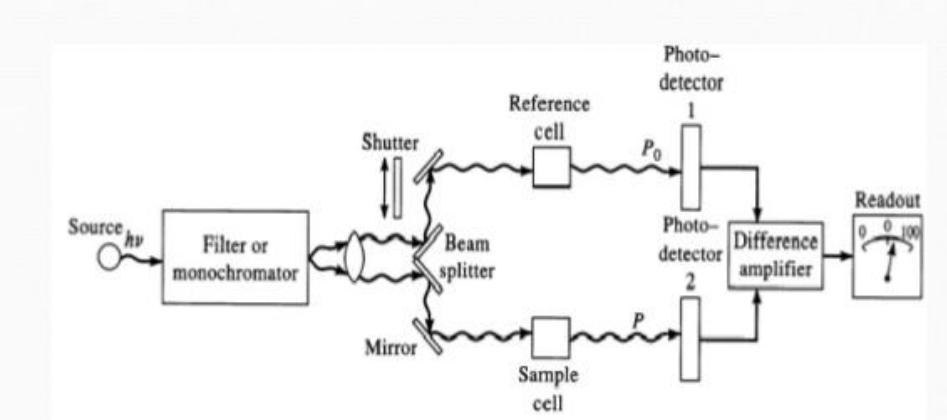

Figure 56: UV-Visible Instrumentation

Principles of Quantitative Spectrometry

Law of Lambert – Beer

When monochromatic radiation passes through the solution containing substance X, which absorbs, the power of radiation decreases progressively along its length due to absorption from substance X. The decrease in power ($P<P_o$) depends on the concentration of substance X and the distance traveled by the beam into the solution. These relations are expressed by the Law of Lambert - Beer, which is usually referred to as the Beer Law and is formulated in the relationship:

$$A = \frac{logPo}{P} = -log\frac{1}{T} = log\left(\frac{100}{\%T}\right) = abc = \varepsilon bc$$

Where:

A= absorbance, P= power of incident radiation, P_o= power of the outgoing radiation, after passing through the solution, T= transmittance, equal with $\frac{P}{Po}$, expressed in percent (% T),it is a clear number, α= ratio constant when c is expressed in gr/L, also called absorbance, b= path length traveled into the solution and is usually expressed in cm, c=concentration of solution, ε= ratio constant when c is expressed in mol / L, also called molar absorption.

The depiction of A or T as the function of wavelength or wavenumber ν, provides the absorption spectrum, which can be used for identifying the existence of functional groups, for clarification of structure the substance it absorbs and identifies. The characteristics of a spectrum are λ_{max} and the corresponding ε_{max}. From absorption A can be found the concentration (c) of the absorbing substance based on the above equation. The wavelength corresponds to the maximum absorption, denoted as λ_{max}, while the minimum absorption corresponds to λ_{min}.

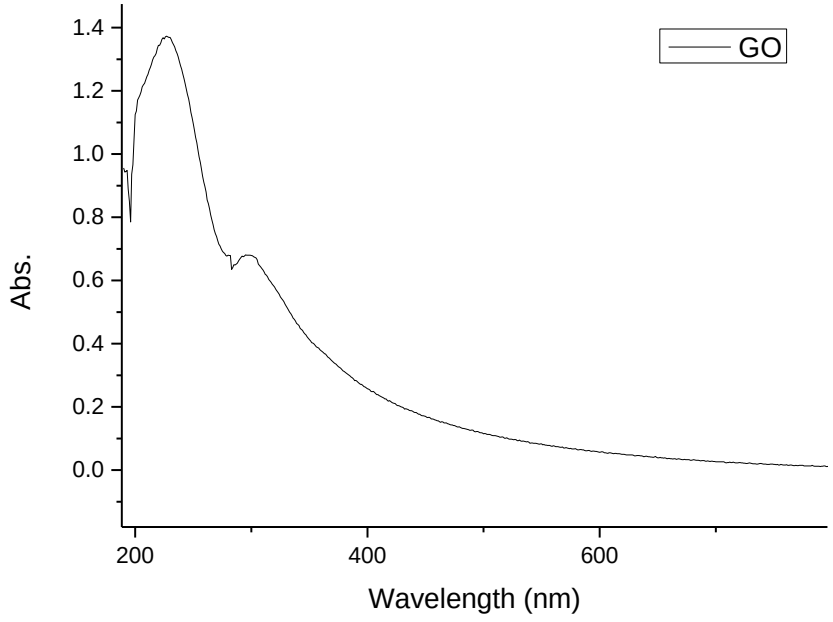

Figure 57: The typical absorption spectrum of GO dispersion

As shown by the above spectrum, the GO has the maximum absorption at 227nm and lower absorption at 297nm. these absorptions, although in small wavelengths, can be

affected the device since the ideal would not be absorbing and all the radiation going at perovskite layer. The peak at 227 nm is due to the transition n-π* antibonding and the peak at 297nm at the basic tranition π-π* bonding orbitals.

6.3.4 Characterization with Atomic Force Microscopy (AFM)

An atomic force microscope is a type of high resolution scanning probe microscope that has a resolution that you can measure in fractions of a nanometer. SPM are designed to measure local properties, such as height, friction, magnetism, with a probe. AFMs operate by measuring force between a probe and the sample. One of the most important tools for imaging on the nanometer scale, Atomic Force Microscopy uses a cantilever with a sharp probe that scans the surface of the sample. When the tip of the probe travels near to a surface, the forces between the tip and sample deflect the cantilever according to Hooke's law. Atomic force microscopy will measure a number of different forces depending on the situation and the sample that you want to measure. As well as the forces, other microscopes can include a probe that performs more specialized measurements, such as temperature. The forces can be classified into attractive and repulsive forces. For attractive forces, van der Waals interaction, electrostatic force and chemical force are included. The chemical forces are described by many different theoretical models. Among them, we can mention Morse potential, Stillinger–Weber potential and Tersoff potential. The repulsive forces can be considered as hard sphere repulsion, Pauli-exclusion interaction and electron–electron Coulomb interaction. The force deflects the cantilever, and this changes the reflection of a laser beams that shines on the top surface of the cantilever onto an array of photodiodes. The variation of the laser beam is a measure of the applied forces. The information is gathered by "feeling" or "touching" the surface with a mechanical probe. Piezoelectric elements that facilitate tiny but accurate and precise movements

on (electronic) command enable precise scanning. For imaging, the reaction of the probe to the forces that the sample imposes on it can be used to form an image of the three-dimensional shape (topography) of a sample surface at a high resolution. This is achieved by raster scanning the position of the sample with respect to the tip and recording the height of the probe that corresponds to a constant probe-sample interaction.

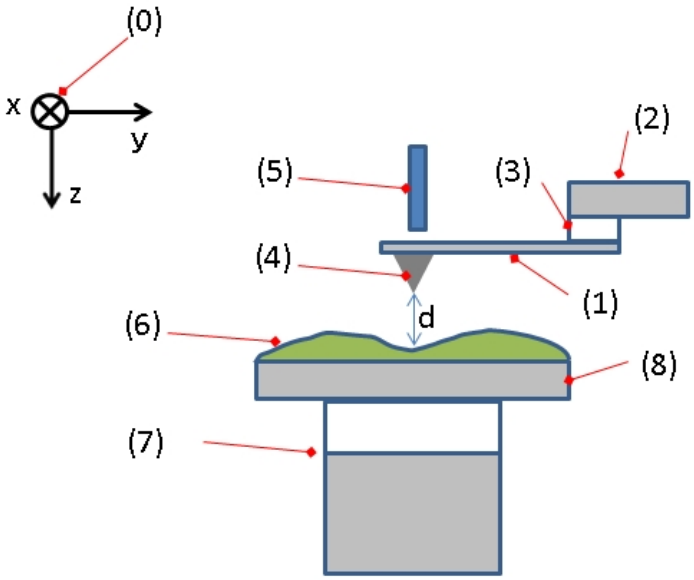

Figure 58: Typical structure of AFM

The instruments of the structure at AFM are:

1. The small cantilever
2. The support for cantilever
3. Piezoelectric element, usually is a ceramic material (to oscillate cantilever at same frequency)
4. The sharp tip fixed to open end of a cantilever, acts as the probe
5. Detector of deflection and motion of the cantilever
6. Sample to be measured by AFM
7. Driver that moves sample at xyz directions with respect to a tip apex
8. The sample stage

Advantages of AFM

The atomic force microscope is a powerful tool that is invaluable if you want to measure incredibly small samples with a great degree of accuracy. it does not require either a vacuum or the sample to undergo treatment that might damage it. At the limits of operation however, researchers have demonstrated atomic resolution in high vacuum and even liquid environments.

Disadvantages of AFM

One of the main is the single scan image size, which is of the order of 150x150 micrometers, compared with millimeters for a scanning electron microscope. Another disadvantage is the relatively slow scan time, which can lead to thermal drift on the sample. As the technology matures, researchers are relying on there being progress instrumentally, requiring improved signal to noise ratio, decreased thermal drift, and better detection and control of tip sample forces, including the use of sharp probes.

Characterization of GO film on substrate with AFM

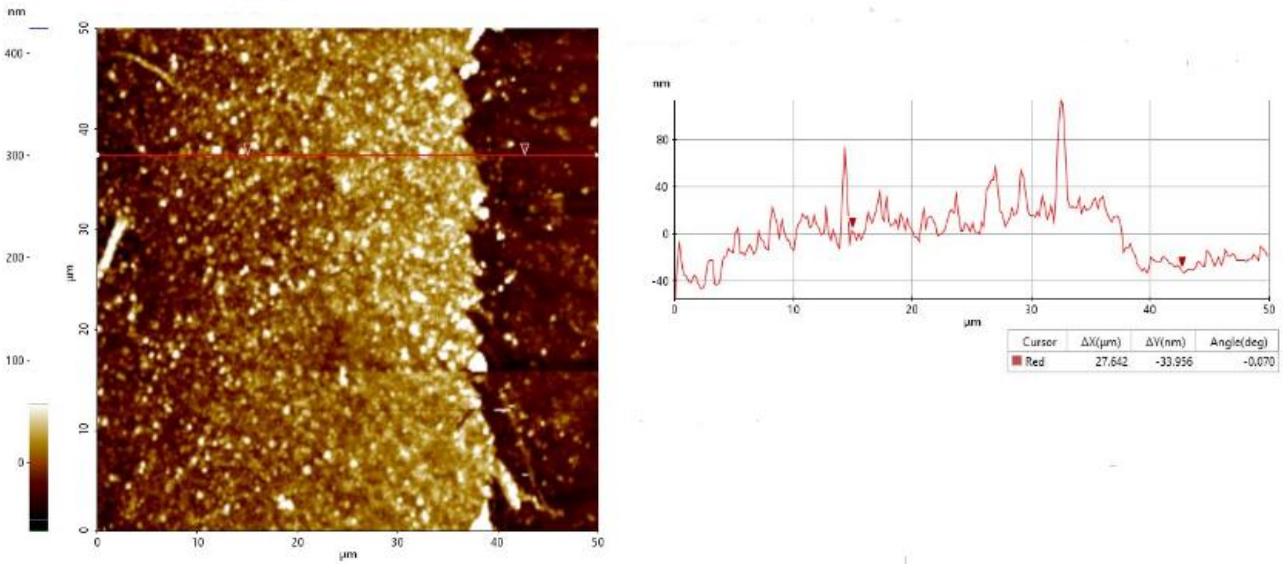

Figure 59: The morphology of the ITO/GO surface with AFM measurement

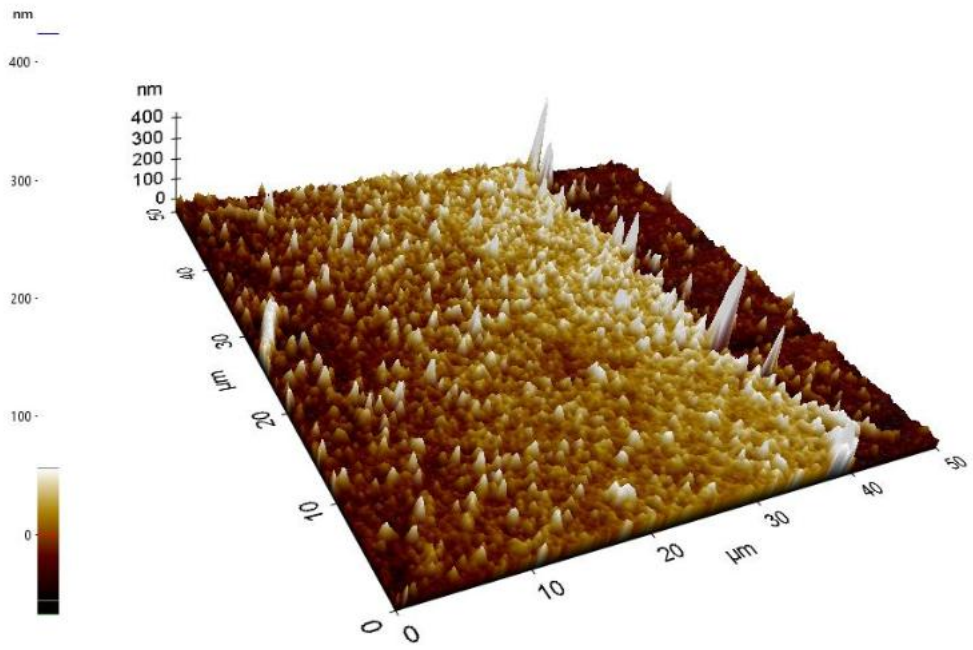

Figure 60: 3D depiction of ITO/GO surface with peaks and curves show the roughness of film

The thickness of GO dispersion was calculated at ~34 nm and the spikes at the layers have roughness at 100nm, that affected the deposition of perovskite layer with result couldn't prepare the device.

7.Introduction of 2D Transition Metal Dichalcogenides (TMDs)

The next big category of 2D materials is Transition Metal Dichalcogenides. Typically, described by the formula MX_2, where M is transition metal (e.g. Mo, W, Nb, Ti, Ta) and X is chalcogenide atom (S, Se, Te) forming X-M-X sheets that are stabilized through weak interactions. Each sheet has an M atom in the middle covalently bonded to six X atoms located at the top and bottom of the sheet. Although the bonding within these sheets is covalent stacked through van der Waals interactions. s. There are more than 40 different types of TMDs having the stoichiometry of MX_2. According to the combination of metal and chalcogenide, the material can be metallic, semi metallic or semiconducting. The main semiconductors of these are: 1) Molybdenum Disulfide (MoS_2), 2) Tungsten Disulfide (WS_2) and 3) Tungsten Diselenide (WSe_2).

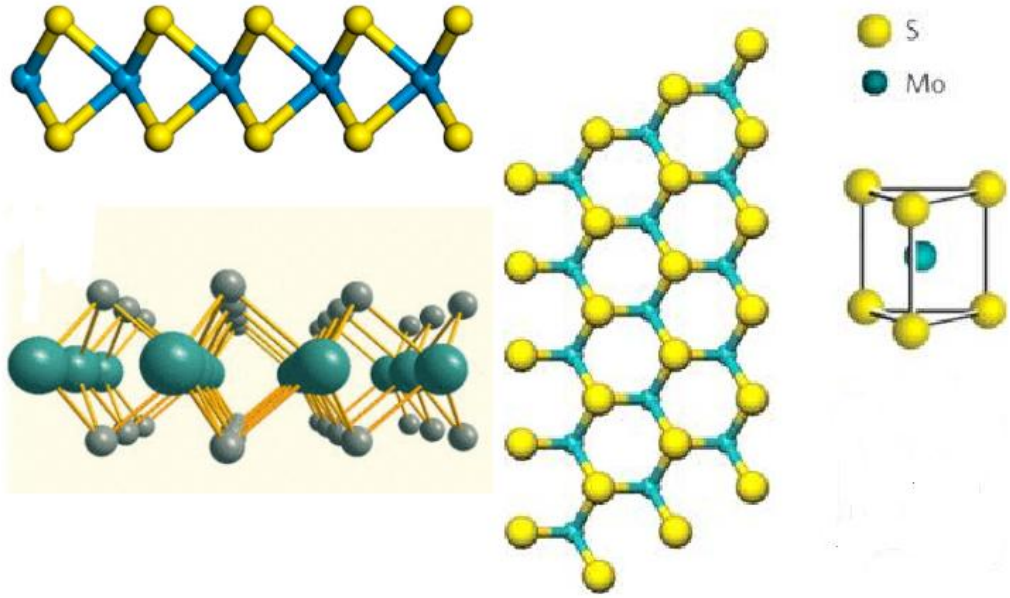

Figure 61: The structure of TMDs: WS2 (left right), WSe2 (left down), MoS2(right)

The applications of TMDs are: super lubricants, materials for batteries, tips for scanning probe microscopes, thin film transistors (TFTs), field effect transistors (FET), enhancement and depletion-mode transistors, light emitting diodes (LEDs), gas sensors, hydrogen evaluation catalyst, bulk heterojunction solar cells and UV range photodetectors.

Single-layer MoS_2 and WS_2 are direct gap semiconductors having bandgap (E_g) of 1.9 and 2.1 eV, respectively, whereas bulk MoS_2 and WS_2 are indirect gap semiconductors having values of Eg of 1.2–1.3 eV.

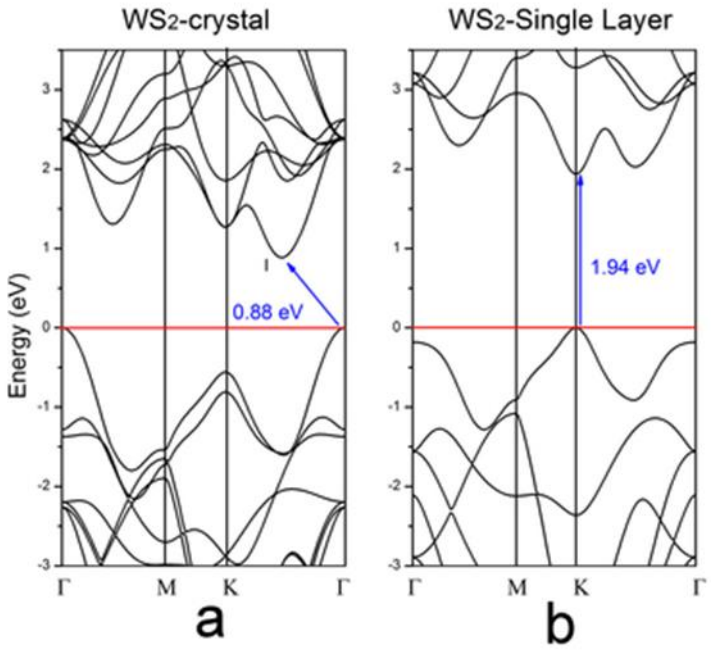

Figure 62: a) Band structure Band structure of bulk hexagonal WS2 (The blue arrow shows the indirect gap Γ-I), (b) Band structure of a monolayer of WS2 (note the blue arrow revealing the direct band gap location

7.1 Synthesis of WS_2 solution

First the powder of WS_2 that used at the laboratory by Graphene supermarket. The created solution of WS_2 had 3.5 mg of powder and 20 ml absolute ethanol. The solution of WS_2 may be sonicated for 6 hours, with the aim to dispersed the bigger flake size and the smaller remain by the solution. This can be achieved with the centrifugation at 1500rpm for 10 sec. After that, was calculated the concentration of final dispersed solution of WS_2, where was it 0.018 mg/ml.

Figure 63: The powder of WS_2

Figure 64: The solution of WS2 flakes

The ***properties*** of WS_2 powder are:

- The purity is 99.0%
- The average of particle size is ~ 90 nm
- The specific surface area is ~30 m^2 /gr
- The color of the solution is silvery and after sonication is done greenish-yellow
- The morphology is nearly spherical
- The solvents useful during sonication include benzyl, isopropanol, acetone, methanol, and many others
- The creation a thin film on the substrate with liquid dispersion used of many applications, such as transistors, solar cells, and energy storage devices
- The VB of WS_2 is 5.75eV and CB is 4.13eV.

The ***properties*** of WS_2 solution are:

- The lateral size is 50-150 nm
- WS_2 flakes are nanoscale crystals dispersed in ethanol/water solution
- Thickness: 1-4 monolayers
- The VB of WS2 is 5.75eV and CB is 4.13eV.
- The purity in dry phase is 99%
- The solution concentration is 26 mg/L and the solution is stable at the ambient conditions
- This solution can be easily deposited at substrate or surface to form a thin

Characterization of WS_2 flakes and solvent ethanol with UV-visible spectroscopy

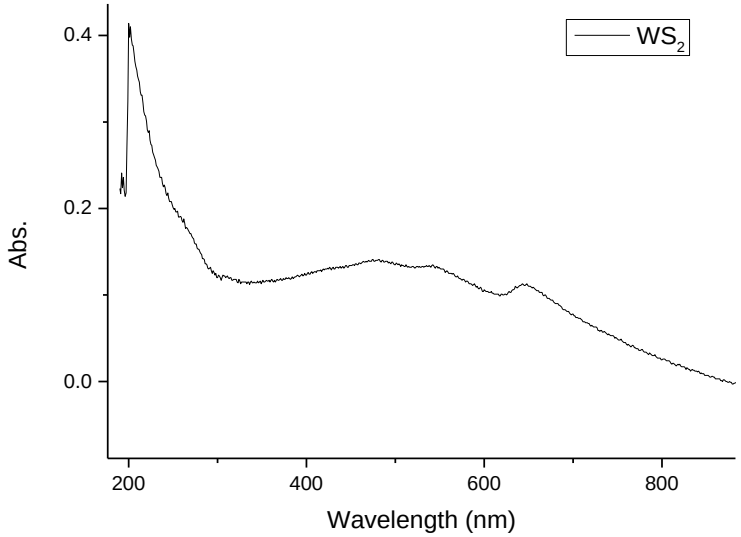

Figure 65: Absorption spectrum of WS_2/ethanol solution

In absorption spectrum were appeared 4 peaks from the material. The first peaks at 201nm was the maximum absorption and smaller at 476nm, 542nm and 645nm, respectively. The first two peaks are due to electron transitions from valance band to the conduction band and the remaining peaks due to the transition from K point to Brillouin Zone.

7.3 Fabrication and Optimization of experimental solar cells

At experimental procedure, were fabricated two structures of solar cells. Firstly, ITO/WS_2/PbI_{2+}MAI/PC_{60}BM/PFN/Ag and ITO/WS_2/$CH_3NH_3PbI_3$/PC_{60}BM/PFN/Ag. The main differences of these devices are:

In first structure used WS_2 solution which prepared in laboratory, the solvent of this solution was absolute ethanol. The deposition of layers was stable at 2000rpm for 40sec with static spin coating. The thermal annealing after the deposition for each layer was 100˚C for 1min and final annealing of substrate with WS_2 layer for 10 secs at hotplate. The deposition of perovskite layer was two step. First, PbI_2 prepared in concentration 450mg/ml DMF and the precursor of MAI was at concentration 45mg/ml anhydrous isopropanol.

For the second structure used the made WS_2 solution from the Graphene supermarket. The solvent of this solution was ethanol/water. The deposition of layers was done optimization from (500-750-1000-1200-1500-2000) rpm for 40 secs with static spin coating. The thermal annealing after the deposition for each layer was 100˚C for 1min and final annealing of substrate with WS_2 layer for 15secs at hotplate, because the solvent had water. The deposition of perovskite was one step with the use of antisolvent diethyl ether. The precursor of perovskite was at a ratio 1:10 DMSO/DMF and 0.05mmols thiourea. The VB of this perovskite is 5.4eV and CB is 3.9eV.

The deposition of remaining layers was done with the same way. The solution of $PC_{60}BM$ was prepared in concentration 20mg/ml chlorobenzene anhydrous and the deposition of this layer was by dynamic spin coating at 1000rpm for 45 secs. The solution of PFN was prepared 0.4mg/ml methanol and 0.3 μl acetic acid and the deposition of PFN was done at 2000rpm for 45 second by dynamic spin coating. The thickness of Ag cathode was at 100nm. At the same time, was fabricated a reference device with structure: ITO/PTAA/PbI_2+MAI/$PC_{60}BM$/PFN/Ag and ITO/PTAA/$CH_3NH_3PbI_3$/$PC_{60}BM$/PFN/Ag to make the comparison of electrical values. In second structure, was fabricated device without HTL to shown the difference between the values. The quantity deposited by WS_2 material was 70μl for each layer.

7.4 Experimental results with characteristics values of solar cells

The device with structure ITO/WS_2/PbI_2+MAI/$PC_{60}BM$/PFN/Ag was given the next electrical characteristic values. The last line was presented the average of these values.

Table 1: Characteristic values from the deposition of 1 layer WS_2

PCE(%)	FF(%)	J_{sc}(mA/cm^2)	Voc(V)
7.33	46.78	19.73	0.79
7.50	47.89	19.78	0.79
7.59	48.11	20.00	0.78

7.45	47.23	20.20	0.78
7.47	**47.50**	**19.93**	**0.78**

Table 2: Characteristic values from the deposition 2 layers of WS_2

PCE(%)	FF(%)	$J_{sc}(mA/cm^2)$	$V_{oc}(V)$
3.63	66.81	7.05	0.77
3.73	67.99	7.09	0.77
3.76	66.48	7.29	0.77
3.77	64.53	7.60	0.77
3.96	**56.85**	**8.95**	**0.77**

Table 3: Characteristic layers from depositing 3 layers of WS_2

PCE(%)	FF(%)	$J_{sc}(mA/cm^2)$	V_{oc} (V)
3.90	78.99	6.66	0.74
3.85	80.05	6.47	0.74
3.76	78.68	6.41	0.74
3.66	77.54	6.32	0.74
3.79	**78.81**	**6.46**	**0.74**

The deposition of 4 layers of WS_2 was not successful, with result to not take electrical measurements.

The first table was presented the deposition for each layers by spin coating. The second device with structure ITO/$CH_3NH_3PbI_3$/PC_{60}BM/PFN/Ag was given the next electrical characteristic values which includes the second following table with the maximum measurement for each solar cell.

Table 5: The deposition rate by spin coating of 1 layer of WS_2

Device	Spin coating
1	500rpm
2	750rpm
3	1200rpm
4	1500rpm
5	2000rpm
6(without HTL)	-

Table 6: Values of fabricated devices

Device	PCE(%)	FF(%)	$J_{sc}(mA/cm^2)$	$V_{oc}(V)$
1	1.26	37.19	5.62	0.57
2	0.72	32.16	4.09	0.52
3	0.41	43.95	3.04	0.29
4	1.20	39.53	5.52	0.56
5	0.80	35.79	3.70	0.57
6	0.31	26.02	2.05	0.56

Table 7: The deposition rate by spin coating of 2 layers of WS_2

Device	Spin coating
1	500rpm
2	750rpm
3	1000rpm
4	1200rpm
5	1500rpm
6	2000rpm

7(without HTL)	-

Only 3 devices were measurable and effective due to short circuit of the device or of non-uniform perovskite layer.

Table 8: Characteristic values of devices

Device	PCE(%)	FF(%)	J_{sc}(mA/cm^2)	V_{oc}(V)
1	1.25	32.10	5.71	0.65
2	1.22	47.59	4.43	0.59
3	0.28	10.43	2.47	0.67

Table 9: The deposition rate by spin coating of 3 layers of WS_2

Device	Spin coating
1	500rpm
2	1000rpm
3	1200rpm
4	1500rpm
5(without HTL)	-

Table 10: Characteristics values

Device	PCE(%)	FF(%)	J_{sc}(mA/cm^2)	V_{oc}(V)
1	1.24	22.56	10.11	0.53
2	0.86	21.87	8.18	0.47

3	0.15	10.10	3.64	0.41
4	1.05	21.78	8.86	0.53
5	0.06	12.90	2.34	0.22

Table 11: The deposition rate by spin coating of 4 layers of WS_2

Device	Spin coating
1	500rpm
2	1000rpm
3	1500rpm
4	2000rpm
5(without HTL)	-

Table 12: Values of fabricated devices

Device	PCE(%)	FF(%)	J_{sc}(Ma/cm^2)	V_{oc}(V)
1	1.25	28.07	9.21	0.47
2	0.76	19.40	8.50	0.45
3	0.81	25.47	7.22	0.43
4	1.00	28.55	6.87	0.50
5	0.42	13.56	6.29	0.48

The reference device with the structure ITO/PTAA/$CH_3NH_3PbI_3$/$PC_{60}BM$/PFN/Ag measured and gave **PCE=13.31%, FF=58.2%, V_{oc}= 0.999V and J_{sc}=21.58 mA/cm^2**

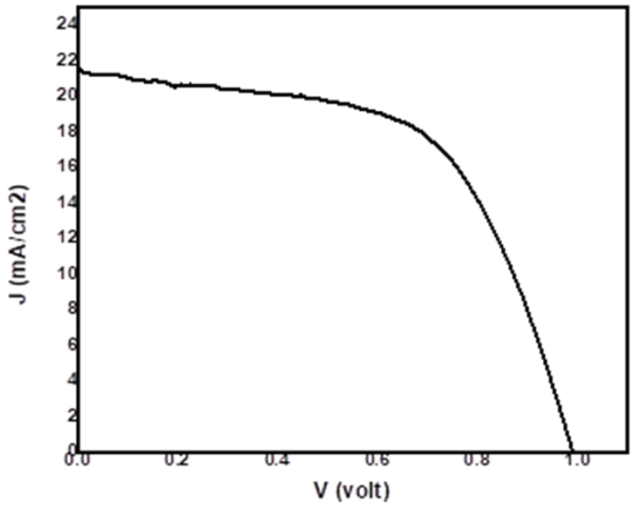

Figure 66: The characteristic curve J-V for the best reference device

7.5 Characterization of WS_2 films on substrate with AFM

To characterize their surface of WS_2 flakes was done optimization for the deposition of these. In the placement of WS_2 flakes from 1 to 5 deposition layers, material appeared in some areas of the substrate. The substrate had ITO/WS_2 for further analysis by AFM.

The thickness of 3 deposition of layers $WS_{2,}$ calculated at around 500nm and meant change of bandgap of material, affecting the electrical properties. For this fabrication and optimization devices until 4 layer $WS_{2.}$ The existence of WS_2 nanosheets was obvious at 3 layers WS_2 at 500rmp by spin coating and presented in the following images.

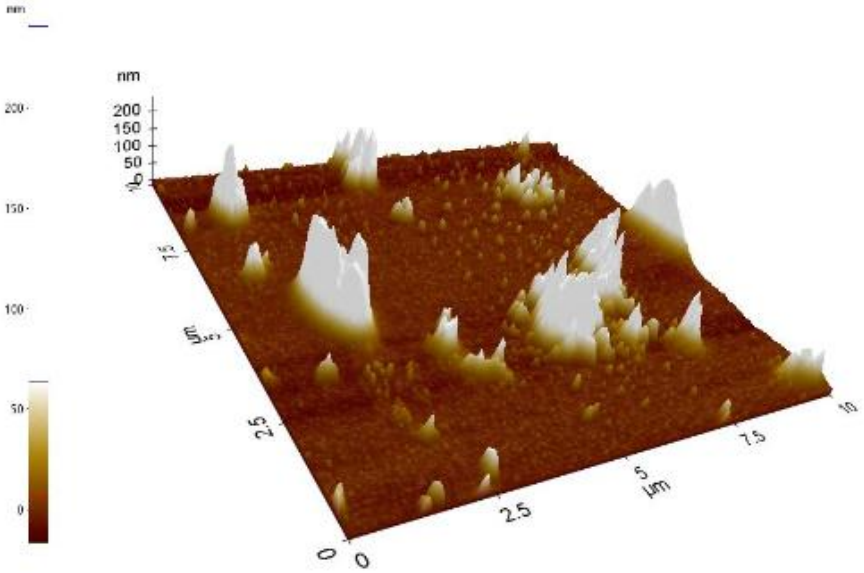

Figure 67: 3D depiction of ITO/WS2 nanosheets surface at substrate

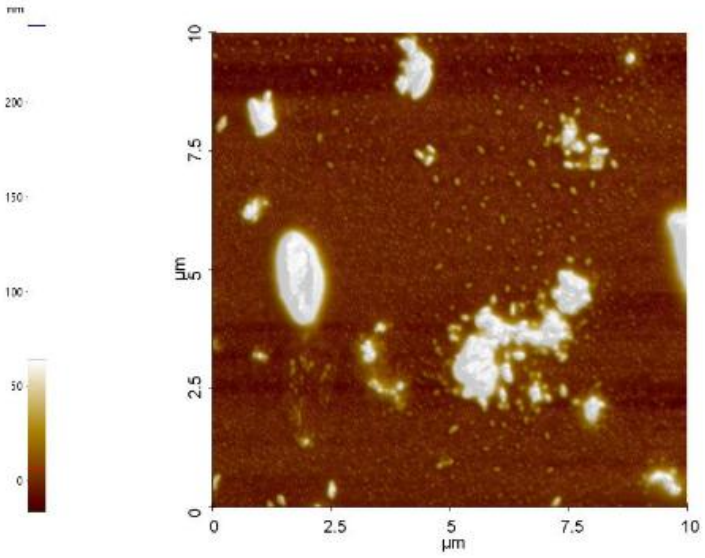

Figure 68: The size of WS2 flakes at the surface of substrate

8.Conclusion

Perovskite solar cells have excellent optoelectronic properties, in just few years have shown tremendous potential for fascinating fundamentals and applied research. Perovskite solar cells have achieved high performance, low cost, easy processing to fabricate devices, directly competing the current state of the art crystalline silicon technology. In this work, was done optimization to fabricate perovskite solar cells. After that changed the HTL at perovskite device from PTAA to GO and WS_2,

selecting these 2D materials because have very significant properties, which affect the performance of perovskite solar cell. Optimization and fabrication was presented particularly. The GO solution fabricated and characterized at the laboratory. Vacuum filtration helped to fabricate GO films and AFM measurement was given the best uniform at thickness of GO. WS_2 solution was used at perovskite solar cell as HTL, depending on the deposition of layers. The higher efficiency was from 1 layer WS_2 deposition 7.47%, fill factor was 47.50%, J_{sc}=19.93(mA/cm^2) and V_{oc}=0.78V, with structure ITO/WS_2/two steps perovskite/ $PC_{60}BM$/PFN/Ag. As shown in AFM, the deposition of WS_2 nanosheets was done at some point of substrate and this resulted the non-uniform device. The best fabricated device with structure ITO/PTAA/$CH_3NH_3PbI_3$ with antisolvent/$PC_{60}BM$/PFN/Ag was measurement PCE=13.31% , Fill Factor was 58.2% V_{oc}=0.99V and J_{sc}=21.58 mA/cm^2.

.

Bibliography

[2] N.-G. Park, “Perovskite solar cells: an emerging photovoltaic technology,” *Mater. Today*, vol. 18, no. 2, pp. 65–72, Mar. 2015.

[3] “Researchers develop world’s most efficient solar cell : Korea.net : The official website of the Republic of Korea.” [Online]. Available: http://www.korea.net/NewsFocus/Sci-Tech/view?articleId=120697. [Accessed: 16-Sep-2018].

[4] S. Adjokatse, H.-H. Fang, and M. A. Loi, “Broadly tunable metal halide perovskites for solid-state light-emission applications,” *Mater. Today*, vol. 20, no. 8, pp. 413–424, Oct. 2017.

[5] S. Brittman, G. W. P. Adhyaksa, and E. C. Garnett, “The expanding world of hybrid perovskites: materials properties and emerging applications,” *MRS Commun.*, vol. 5, no. 01, pp. 7–26, Mar. 2015.

[6] Y.-C. Hsiao, T. Wu, M. Li, Q. Liu, W. Qin, and B. Hu, “Fundamental physics behind high-efficiency organo-metal halide perovskite solar cells,” *J. Mater. Chem. A*, vol. 3, no. 30, pp. 15372–15385, 2015.

[7] Y. Li *et al.*, “Direct Observation of Long Electron-Hole Diffusion Distance in CH3NH3PbI3 Perovskite Thin Film,” *Sci. Rep.*, vol. 5, no. 1, p. 14485, Nov. 2015.

[8] A. Babayigit, A. Ethirajan, M. Muller, and B. Conings, “Toxicity of organometal halide perovskite solar cells,” *Nat. Mater.*, vol. 15, no. 3, pp. 247–251, Mar. 2016.

[9] D. Wang, M. Wright, N. K. Elumalai, and A. Uddin, “Stability of perovskite solar cells,” *Sol. Energy Mater. Sol. Cells*, vol. 147, pp. 255–275, Apr. 2016.

[10] G. A. Nemnes *et al.*, “Normal and Inverted Hysteresis in Perovskite Solar Cells,” *J. Phys. Chem. C*, vol. 121, no. 21, pp. 11207–11214, Jun. 2017.

[11] N. Elumalai *et al.*, “Perovskite Solar Cells: Progress and Advancements,” *Energies*, vol. 9, no. 11, p. 861, Oct. 2016.

[12] “Photovoltaic Solar Cell Turns Photons into Electrons.” [Online]. Available: http://www.alternative-energy-tutorials.com/energy-articles/solar-cell-turns-photons-into-electrons.html. [Accessed: 21-Sep-2018].

[13] E. Edri, S. Kirmayer, S. Mukhopadhyay, K. Gartsman, G. Hodes, and D. Cahen, “Elucidating the charge carrier separation and working mechanism of CH3NH3PbI3−xCl x perovskite solar cells,” *Nat. Commun.*, vol. 5, no. 1, p. 3461, Dec. 2014.

[14] P. Gao, M. Grätzel, and M. K. Nazeeruddin, “Organohalide lead perovskites for photovoltaic applications,” *Energy Environ. Sci.*, vol. 7, no. 8, pp. 2448–2463, Jul. 2014.

[15] R. Steim, F. R. Kogler, and C. J. Brabec, “Interface materials for organic solar cells,” *J. Mater. Chem.*, vol. 20, no. 13, p. 2499, Mar. 2010.

[16] L. Łukasiak and A. Jakubowski, “History of Semiconductors,” *J. Telecommun.*

Inf. Technol., p. 3, 2010.

[17] "Solar Cell I-V Characteristic and Solar I-V Curves." [Online]. Available: http://www.alternative-energy-tutorials.com/energy-articles/solar-cell-i-v-characteristic.html. [Accessed: 22-Sep-2018].

[18] "Quantum Efficiency | PVEducation." [Online]. Available: https://www.pveducation.org/pvcdrom/solar-cell-operation/quantum-efficiency. [Accessed: 22-Sep-2018].

[19] X. Zhao and M. Wang, "Organic hole-transporting materials for efficient perovskite solar cells," *Mater. Today Energy*, vol. 7, pp. 208–220, 2018.

[20] Z. H. Bakr, Q. Wali, A. Fakharuddin, L. Schmidt-Mende, T. M. Brown, and R. Jose, "Advances in hole transport materials engineering for stable and efficient perovskite solar cells," *Nano Energy*, vol. 34, no. November 2016, pp. 271–305, 2017.

[21] J. Lian, B. Lu, F. Niu, P. Zeng, and X. Zhan, "Electron-Transport Materials in Perovskite Solar Cells," *Small Methods*, vol. 1800082, p. 1800082, 2018.

[22] J. H. Heo *et al.*, "Efficient inorganic-organic hybrid heterojunction solar cells containing perovskite compound and polymeric hole conductors," *Nat. Photonics*, vol. 7, no. 6, pp. 486–491, 2013.

[23] Z. He, C. Zhong, S. Su, M. Xu, H. Wu, and Y. Cao, "Enhanced power-conversion efficiency in polymer solar cells using an inverted device structure," *Nat. Photonics*, vol. 6, no. 9, pp. 591–595, 2012.

[24] D. Lidzey, "Engineering low-cost energy from plastic photovoltaics," *SPIE Newsroom*, 2009.

[25] "physical vapor deposition| vacuum chamber| thin layer| coating| surface engineering| titanium coating| sputter coating| ion plating| vacuum evaporation| vaporization| resistance heater| mechanical manipulator| deposition| bombarding| cathode| cathodic coa." [Online]. Available: http://www.mechscience.com/physical-vapor-deposition/. [Accessed: 17-Sep-2018].

[26] C. Liu, Z. Yu, D. Neff, A. Zhamu, and B. Z. Jang, "Graphene-Based Supercapacitor with an Ultrahigh Energy Density," *Nano Lett.*, vol. 10, no. 12, pp. 4863–4868, Dec. 2010.

[27] K. S. Novoselov, V. I. Fal′ko, L. Colombo, P. R. Gellert, M. G. Schwab, and K. Kim, "A roadmap for graphene," *Nature*, vol. 490, no. 7419, pp. 192–200, Oct. 2012.

[28] † Michael J. McAllister *et al.*, "Single Sheet Functionalized Graphene by Oxidation and Thermal Expansion of Graphite," 2007.

[29] N. I. Zaaba, K. L. Foo, U. Hashim, S. J. Tan, W.-W. Liu, and C. H. Voon, "Synthesis of Graphene Oxide using Modified Hummers Method: Solvent Influence," *Procedia Eng.*, vol. 184, pp. 469–477, 2017.

[30] T. Viet Cuong *et al.*, "Temperature-dependent photoluminescence from chemically and thermally reduced graphene oxide," *Appl. Phys. Lett.*, vol. 99, no. 4, p. 041905, Jul. 2011.

[31] X. Gao, J. Jang, and S. Nagase, "Hydrazine and Thermal Reduction of Graphene Oxide: Reaction Mechanisms, Product Structures, and Reaction Design," *J. Phys. Chem. C*, vol. 114, no. 2, pp. 832–842, Jan. 2010.

[32] A. Watanabe and J. Cai, "Laser direct writing of reduced graphene oxide micropatterns and sensor applications," in *Laser-based Micro- and Nanoprocessing XII*, 2018, vol. 10520, p. 27.

[33] Q.-D. Yang‡ *et al.*, "Graphene oxide as an efficient hole-transporting material for high-performance perovskite solar cells with enhanced stability," *J. Mater. Chem. A*, vol. 5, no. 20, pp. 9852–9858, 2017.

[34] S. Rafique, S. M. Abdullah, M. M. Shahid, M. O. Ansari, and K. Sulaiman, "Significantly improved photovoltaic performance in polymer bulk heterojunction solar cells with graphene oxide /PEDOT:PSS double decked hole transport layer," *Sci. Rep.*, vol. 7, no. September 2016, pp. 1–10, 2017.

[35] H. Wang *et al.*, "Multifunctional TiO2nanowires-modified nanoparticles bilayer film for 3D dye-sensitized solar cells," *Optoelectron. Adv. Mater. Rapid Commun.*, vol. 4, no. 8, pp. 1166–1169, 2010.

[36] "MF-Millipore™ MCE Membrane Filters | Sigma-Aldrich." [Online]. Available: https://www.sigmaaldrich.com/technical-documents/articles/biology/mf-millipore-mce-membrane-filters.html. [Accessed: 19-Sep-2018].

[37] N. J. Jeon, J. H. Noh, Y. C. Kim, W. S. Yang, S. Ryu, and S. Il Seok, "Solvent engineering for high-performance inorganic–organic hybrid perovskite solar cells," *Nat. Mater.*, vol. 13, no. 9, pp. 897–903, Sep. 2014.

[38] "Ultraviolet-Visible (UV-Vis) Spectroscopy | Analytical Chemistry | PharmaXChange.info." [Online]. Available: https://pharmaxchange.info/2011/12/ultraviolet-visible-uv-vis-spectroscopy-principle/. [Accessed: 19-Sep-2018].

[39] "UV Visible Spectroscopy." [Online]. Available: https://www.slideshare.net/aviforu12/seminar-uv-visible-spectroscopy. [Accessed: 19-Sep-2018].

[40] "absorption spectra - the Beer-Lambert Law." [Online]. Available: https://www.chemguide.co.uk/analysis/uvvisible/beerlambert.html. [Accessed: 19-Sep-2018].

[41] G. Binnig, C. F. Quate, and C. Gerber, "Atomic force microscope.," *Phys. Rev. Lett.*, vol. 56, no. 9, pp. 930–933, Mar. 1986.

[42] "The Atomic Force Microscope (AFM), What are its Uses in Microscopy Today." [Online]. Available: https://www.microscopemaster.com/atomic-force-microscope.html. [Accessed: 21-Sep-2018].

[43] W. Choi, N. Choudhary, G. H. Han, J. Park, D. Akinwande, and Y. H. Lee, "Recent development of two-dimensional transition metal dichalcogenides and their applications," *Mater. Today*, vol. 20, no. 3, pp. 116–130, Apr. 2017.

[44] E. Lassner and W.-D. Schubert, *Tungsten : properties, chemistry, technology of the element, alloys, and chemical compounds*. Kluwer Academic/Plenum Publishers, 1999.

[45] M. A. Ibrahem *et al.*, "High quantity and quality few-layers transition metal disulfide nanosheets from wet-milling exfoliation," *RSC Adv.*, vol. 3, no. 32, pp. 13193–13202, 2013.

[46] R. Ganatra and Q. Zhang, "Few-Layer MoS $_2$: A Promising Layered Semiconductor," *ACS Nano*, vol. 8, no. 5, pp. 4074–4099, May 2014.

[47] K.-K. Kam, "Electrical properties of WSe2, WS2, MoSe2, MoS2, and their use as photoanodes in a semiconductor liquid junction solar cell," 1982.

[48] H. Terrones, F. López-Urías, and M. Terrones, "Novel hetero-layered materials with tunable direct band gaps by sandwiching different metal disulfides and diselenides.," *Sci. Rep.*, vol. 3, p. 1549, 2013.

[49] "Graphene Supermarket." [Online]. Available: https://graphene-supermarket.com/home.php. [Accessed: 22-Sep-2018].